NATIONAL ADVISORY COMMITTEE FOR AERONAUTICS

REPORT 1001

FUNDAMENTAL EFFECTS OF AGING ON CREEP PROPERTIES OF SOLUTION-TREATED LOW-CARBON N-155 ALLOY

By D. N. FREY, J. W. FREEMAN, and A. E. WHITE



1950

For sale by the Superintendent of Documents, U. S. Government Printing Office, Washington 25, D. C. Yearly subscription, $3.50; foreign, $4.50; single copy price varies according to size. - - - - - - - - - Price 25 cents

AERONAUTIC SYMBOLS

1. FUNDAMENTAL AND DERIVED UNITS

	Symbol	Metric		English	
		Unit	Abbreviation	Unit	Abbreviation
Length	l	meter	m	foot (or mile)	ft (or mi)
Time	t	second	s	second (or hour)	sec (or hr)
Force	F	weight of 1 kilogram	kg	weight of 1 pound	lb
Power	P	horsepower (metric)		horsepower	hp
Speed	V	kilometers per hour	kph	miles per hour	mph
		meters per second	mps	feet per second	fps

2. GENERAL SYMBOLS

W Weight$=mg$

g Standard acceleration of gravity$=9.80665$ m/s^2 or 32.1740 ft/sec^2

m Mass$=\frac{W}{g}$

I Moment of inertia$=mk^2$. (Indicate axis of radius of gyration k by proper subscript.)

μ Coefficient of viscosity

ν Kinematic viscosity

ρ Density (mass per unit volume)

Standard density of dry air, 0.12497 kg-m^{-4}-s^2 at 15° C and 760 mm; or 0.002378 lb-ft^{-4} sec^2

Specific weight of "standard" air, 1.2255 kg/m^3 or 0.07651 lb/cu ft

3. AERODYNAMIC SYMBOLS

S Area

S_w Area of wing

G Gap

b Span

c Chord

A Aspect ratio, $\frac{b^2}{S}$

V True air speed

q Dynamic pressure, $\frac{1}{2}\rho V^2$

L Lift, absolute coefficient $C_L=\frac{L}{qS}$

D Drag, absolute coefficient $C_D=\frac{D}{qS}$

D_0 Profile drag, absolute coefficient $C_{D_0}=\frac{D_0}{qS}$

D_i Induced drag, absolute coefficient $C_{D_i}=\frac{D_i}{qS}$

D_p Parasite drag, absolute coefficient $C_{D_p}=\frac{D_p}{qS}$

C Cross-wind force, absolute coefficient $C_C=\frac{C}{qS}$

i_w Angle of setting of wings (relative to thrust line)

i_t Angle of stabilizer setting (relative to thrust line)

Q Resultant moment

Ω Resultant angular velocity

R Reynolds number, $\rho\frac{Vl}{\mu}$ where l is a linear dimension (e.g., for an airfoil of 1.0 ft chord, 100 mph, standard pressure at 15° C, the corresponding Reynolds number is 935,400; or for an airfoil of 1.0 m chord, 100 mps, the corresponding Reynolds number is 6,865,000)

α Angle of attack

ϵ Angle of downwash

α_0 Angle of attack, infinite aspect ratio

α_i Angle of attack, induced

α_a Angle of attack, absolute (measured from zero-lift position)

γ Flight-path angle

REPORT 1001

FUNDAMENTAL EFFECTS OF AGING ON CREEP PROPERTIES OF SOLUTION-TREATED LOW-CARBON N-155 ALLOY

By D. N. FREY, J. W. FREEMAN, and A. E. WHITE

University of Michigan

National Advisory Committee for Aeronautics

Headquarters, 1724 F Street NW., Washington 25, D. C.

Created by act of Congress approved March 3, 1915, for the supervision and direction of the scientific study of the problems of flight (U. S. Code, title 50, sec. 151). Its membership was increased from 12 to 15 by act approved March 2, 1929, and to 17 by act approved May 25, 1948. The members are appointed by the President, and serve as such without compensation.

JEROME C. HUNSAKER, Sc. D., Massachusetts Institute of Technology, *Chairman*

ALEXANDER WETMORE, Sc. D., Secretary, Smithsonian Institution, *Vice Chairman*

DETLEV W. BRONK, PH. D., President, Johns Hopkins University.

JOHN H. CASSADY, Vice Admiral, United States Navy, Deputy Chief of Naval Operations.

EDWARD U. CONDON, PH. D., Director, National Bureau of Standards.

HON. THOMAS W. S. DAVIS, Assistant Secretary of Commerce.

JAMES H. DOOLITTLE, Sc. D., Vice President, Shell Union Oil Corp.

R. M. HAZEN, B. S., Director of Engineering, Allison Division, General Motors Corp.

WILLIAM LITTLEWOOD, M. E., Vice President, Engineering, American Airlines, Inc.

THEODORE C. LONNQUEST, Rear Admiral, United States Navy, Deputy and Assistant Chief of the Bureau of Aeronautics.

DONALD L. PUTT, Major General, United States Air Force, Director of Research and Development, Office of the Chief of Staff, Development.

ARTHUR E. RAYMOND, Sc. D., Vice President, Engineering, Douglas Aircraft Co., Inc.

FRANCIS W. REICHELDERFER, Sc. D., Chief, United States Weather Bureau.

HON. DELOS W. RENTZEL, Administrator of Civil Aeronautics, Department of Commerce.

GORDON P. SAVILLE, Major General, United States Air Force, Deputy Chief of Staff—Development.

WILLIAM WEBSTER, M. S., Chairman, Research and Development Board, Department of Defense.

THEODORE P. WRIGHT, Sc. D., Vice President for Research, Cornell University.

HUGH L. DRYDEN, PH. D., *Director*

JOHN F. VICTORY, LL. D., *Executive Secretary*

JOHN W. CROWLEY, JR., B. S., *Associate Director for Research*

E. H. CHAMBERLIN, *Executive Officer*

HENRY J. E. REID, D. Eng., Director, Langley Aeronautical Laboratory, Langley Field, Va.

SMITH J. DEFRANCE, B. S., Director, Ames Aeronautical Laboratory, Moffett Field, Calif.

EDWARD R. SHARP, Sc. D., Director, Lewis Flight Propulsion Laboratory, Cleveland Airport, Cleveland, Ohio

---

TECHNICAL COMMITTEES

AERODYNAMICS
POWER PLANTS FOR AIRCRAFT
AIRCRAFT CONSTRUCTION
OPERATING PROBLEMS
INDUSTRY CONSULTING

Coordination of Research Needs of Military and Civil Aviation
Preparation of Research Programs
Allocation of Problems
Prevention of Duplication
Consideration of Inventions

LANGLEY AERONAUTICAL LABORATORY, Langley Field, Va.

LEWIS FLIGHT PROPULSION LABORATORY, Cleveland Airport, Cleveland, Ohio

AMES AERONAUTICAL LABORATORY, Moffett Field, Calif.

Conduct, under unified control, for all agencies, of scientific research on the fundamental problems of flight

---

OFFICE OF AERONAUTICAL INTELLIGENCE,
Washington, D. C.

Collection, classification, compilation, and dissemination of scientific and technical information on aeronautics

REPORT 1001

FUNDAMENTAL EFFECTS OF AGING ON CREEP PROPERTIES OF SOLUTION-TREATED LOW-CARBON N–155 ALLOY[1]

By D. N. Frey, J. W. Freeman, and A. E. White

SUMMARY

A method is developed whereby the fundamental mechanisms are investigated by which processing, heat treatment, and chemical composition control the properties of alloys at high temperatures. This method uses metallographic examination—both optical and electronic—studies of X-ray diffraction-line widths, intensities, and lattice parameters, and hardness surveys to evaluate fundamental structural conditions. Mechanical properties at high temperatures are then measured and correlated with these measured structural conditions.

In accordance with this method, a study was made of the fundamental mechanism by which aging controlled the short-time creep and rupture properties of solution-treated low-carbon N–155 alloy at 1200° F. The test stock was solution-treated at 2200° F for 10 hours, water-quenched, and aged for time periods up to 1000 hours at 1200°, 1400°, and 1600° F.

Correlation of the structural effects of aging with the mechanical properties indicated that aging had the following effects on solution-treated low-carbon N–155 alloy:

(1) *Aging resulted in progressive lowering of short-time creep resistance through removal from solid solution of large-radius or substitutional atoms by precipitation.*

(2) *Short-time aging resulted in marked increase in short-time rupture strengths through the growth of a grain boundary phase which eliminated intergranular cracking. Long-time aging resulted in little further change in short-time rupture strength.*

(3) *Because aging lowered the creep resistance while raising the rupture strength, aged material exhibited greater ductility before fracture than unaged material.*

Calculations are carried out to show the probable character of the strain field induced in the solution-treated state by the presence of the large-radius atoms—molybdenum, tungsten, and columbium—and the substitutional atoms—nitrogen and carbon. The effect of this strain field on the creep resistance is also considered quantitatively.

These findings, however, should not be considered generally applicable to long-time strength, to strength at other temperatures, or to the same alloy in other conditions of treatment. In order to develop a general theory of high-temperature strength, additional data on other alloys and on the same alloy in the other conditions will have to be gathered.

INTRODUCTION

This report covers the first part of a continuing investigation into the fundamental behavior at high temperatures of austenitic alloys designed for use in aircraft propulsion systems. Previous investigation (e. g., see reference 1) has shown in part the effects of prior processing and heat-treatment conditions on the high-temperature properties of low-carbon N–155 alloy and various other austenitic high-temperature alloys. In order to develop better and practicable alloys on a scientific basis, to utilize critical materials to the fullest possible extent, and to point out logical methods of production control for uniform properties, more knowledge must be gained of the fundamental reasons for the high-temperature behavior of austenitic high-temperature alloys.

The basic assumption of the investigation was that the behavior of certain alloys at high temperature is dependent on their microstructure and the lattice conditions of the matrix. The experimental program was therefore designed to measure first these two characteristics of one alloy, low-carbon N–155, as influenced by heat treatment, chemical composition, and exposure to temperature and stress. Optical- and electron-microscope techniques and separation and analysis of microconstituents were used to define structural conditions. The lattice conditions of the matrix, particularly the strains present, were measured by X-ray diffraction techniques. Second, the creep and rupture properties, corresponding to these structural conditions, were established. Third, these data were then correlated and interpreted using the fundamentals of physics of solids and plastic flow to as great an extent as possible.

It was felt that by concentrating at first wholly on one particular alloy, the thorough understanding thus gained could be best generalized for extension to other alloys. The experimental variations which necessarily had to be covered require a prohibitive amount of work for even two alloys. Low-carbon N–155 alloy was chosen primarily because it was a representative alloy of a type important in the aircraft propulsion field. In addition, there was a considerable background of experimental data for this alloy which would be of value to the investigation.

This report presents the results obtained to date on bar-stock material, solution-treated at 2200° F for 10 hours and aged for time periods up to 1000 hours at 1200°, 1400°, and 1600° F. The creep and rupture data were confined to short time periods at 1200° F under a restricted stress range.

[1] Supersedes NACA TN 1940, "Fundamental Effects of Aging on Creep Properties of Solution-Treated Low-Carbon N–155 Alloy" by D. N. Frey, J. W. Freeman, and A. E. White, 1949.

This is, therefore, in the nature of a report on the techniques developed and progress made to date. A large amount of additional experimental work must be done before all temperatures, stresses, and time periods of interest are related to the structural conditions of the alloy resulting from the wide range of possible prior treatment.

The investigation is part of a research program on heat-resistant alloys for aircraft propulsion systems conducted at the Engineering Research Institute of the University of Michigan under the sponsorship and with the financial assistance of the National Advisory Committee for Aeronautics.

TEST MATERIALS

Low-carbon N–155 alloy bar stock was used in this investigation. It represents part of the complete product of one ingot of heat A–1726 rolled into the ⅞-inch broken-corner square stock. Each bar from the ingot was numbered so that its position relative to the original ingot was known. The particular material considered herein came from the center of the ingot.

The composition of heat A–1726 reported by the supplier is listed as follows, together with the results of the analysis by the university of the bar from the center of the particular ingot being considered:

Source of analysis	Chemical composition (percent)									
	C	Mn	Si	Cr	Ni	Co	Mo	W	Cb	N
Supplier's heat analysis	0.13	1.63	0.42	21.22	19.00	19.70	2.90	2.61	0.84	0.13
Bar from center of ingot (Univ. of Mich.)	.133	1.43	.34	20.73	18.92	19.65	3.05	1.98	.98	.14

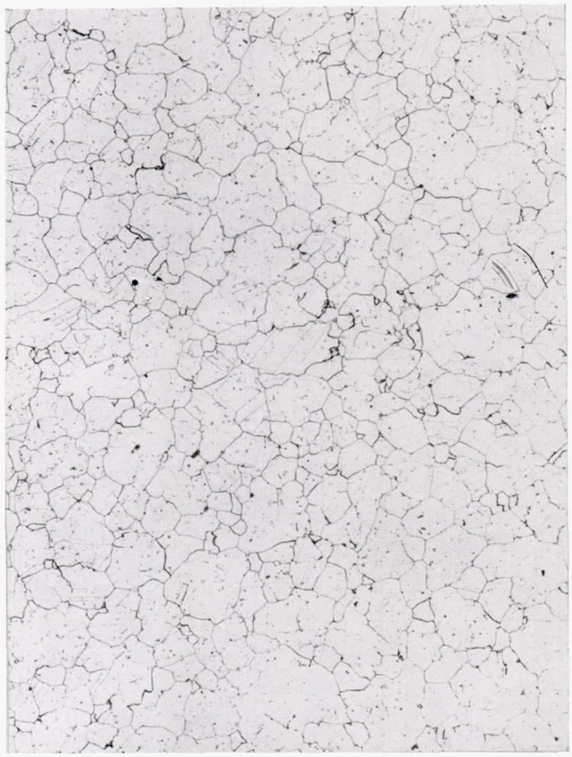
The appendix gives the complete processing schedule reported for the ingot of heat A–1726 from which the test stock was taken.

Prior to use, the stock for this investigation was solution-treated 10 hours at 2200° F and water-quenched. The solution treatment was made unusually long for the purpose of distributing the precipitant atoms randomly in the matrix and so that internal strain, due to the prior working of the material, would be reduced to a very low level.

Moderate grain growth took place over the major portion of the bar cross section during the 10-hour treatment, but on two diagonally opposite corners pronounced growth took place. A hardness survey of the as-rolled bar stock showed the average hardness across one diagonal to be higher than across the other; from this the conclusion may be drawn that the rolling operation had worked the bar across one diagonal preferentially. All mechanical testing and physical measure-



(*a*) As rolled.



(*b*) Solution-treated 10 hours at 2200° F, water-quenched, and aged 1 hour at 1400° F.

FIGURE 1.—Typical microstructures of heat A–1726 of low-carbon N–155 alloy. Small-grained area. Cross sections of bar, X100. Electrolytically etched in 10 percent chromic acid.

ments were restricted to the fine-grained section of the bar stock. Figure 1 shows representative structures of the cross section of the bar stock as rolled and after the 10-hour solution treatment.

EXPERIMENTAL PROCEDURES

The general procedure was to age the solution-treated stock at selected temperatures and time periods and then to carry out the microstructural studies and X-ray diffraction measurements in order to establish the structural characteristics resulting from the aging treatments. The strength properties resulting from the aging treatments were measured for short time periods at 1200° F. These experiments were intended to establish the relationship between short-time creep and rupture properties and nucleation, precipitation, and precipitate particle size and distribution during aging.

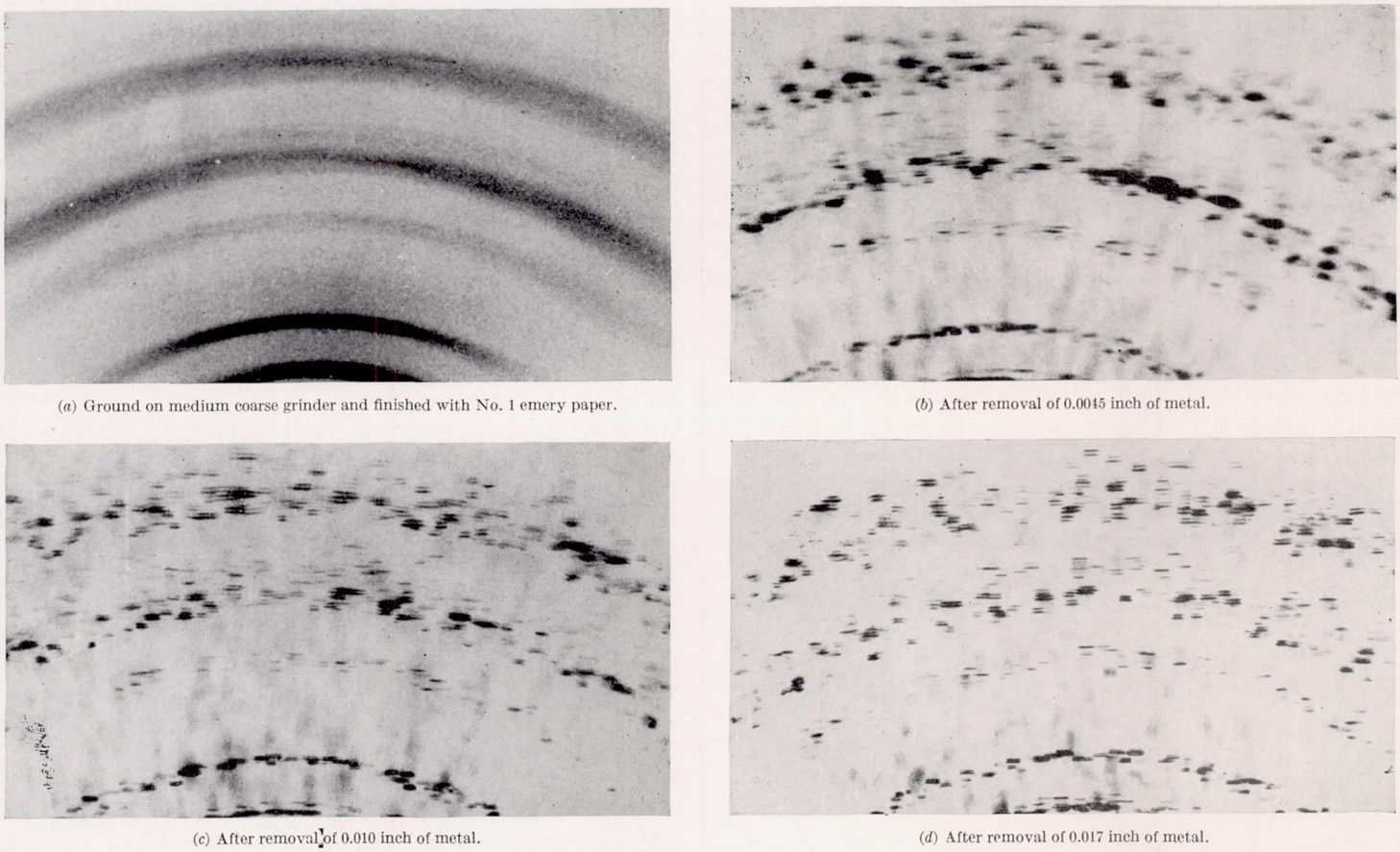
The details of the experimental procedures are described in the following sections.

AGING

Aging treatments were carried out at 1200°, 1400°, and 1600° F for time periods of 1, 10, 100, and 1000 hours and such other intermediate times as became necessary. The samples were heated in small automatically controlled muffle furnaces in an air atmosphere. These furnaces were at temperature when samples were placed in them and the time period of heating was considered started after the specimens had been in the furnace for ¼ hour. After aging, all samples were air-cooled. Sufficient stock was aged at each condition for the microstructural, X-ray, and mechanical tests.

OPTICAL-MICROSCOPE STUDIES

After aging, the individual samples were ground on a cross-sectional face, polished with No. 1 emery cloth, Nos. 1, 1/0, 2/0, and 3/0 emery papers, transferred to a cloth disk, polished using a commercial chromium buffing compound, and finished on a Gamal wet wheel; they were then electrolytically



(*a*) Ground on medium coarse grinder and finished with No. 1 emery paper.

(*b*) After removal of 0.0045 inch of metal.

(*c*) After removal of 0.010 inch of metal.

(*d*) After removal of 0.017 inch of metal.

FIGURE 2.—Diffraction patterns showing removal by electrolytic polishing of cold-worked surface on low-carbon N–155 alloy solution-treated 10 hours at 2200° F and water-quenched. Unfiltered molybdenum radiation (55 kv).

etched for 5 seconds in 10 percent chromic acid at 1 ampere per square inch. After study under a microscope, representative photomicrographs were taken of each sample at 1000 diameters under slightly oblique illumination.

ELECTRON-MICROSCOPE STUDIES

In order to obtain electron micrographs from metallographic samples, replicas which will transmit the electron stream must be prepared of the surfaces. For the investigations reported herein, Formvar replicas were prepared according to the technique outlined in reference 2. The metallographic surfaces from which these replicas were prepared were the same polished and etched surfaces photographed optically. The replicas (shadow-cast with chromium) were then mounted in an RCA Model B electron microscope and photographs taken at approximately 3000X. Enlargement to 8500X was done photographically.

X-RAY STUDIES

Sample preparation.—A great deal of difficulty with variable and unreproducible diffraction data was initially encountered. The difficulty was found to be due to both mechanically disturbed metal surfaces and unrandom grain orientation. Eventually the development of the following technique produced results sufficiently free from these difficulties for this investigation:

(1) A layer of metal 0.020 inch thick was electrolytically removed from the surface of all samples which were used for X-ray analysis. The amount of metal which had to be removed in order to get below the artificially strained surfaces produced by a cut-off wheel, by grinding, or as a result of metallographic polishing was determined by X-ray diffraction patterns of the type shown by figure 2 and made by the apparatus illustrated in figure 3. The patterns in figure 2, taken from a surface initially ground, show the emergence of the reflections of the individual grains and finally resolution of the $\alpha_1\alpha_2$ doublet of the molybdenum K radiation with increasing depth of metal removal. The amount of surface removal shown in figure 2 as necessary to obtain a strain-free surface was typical for all samples used.

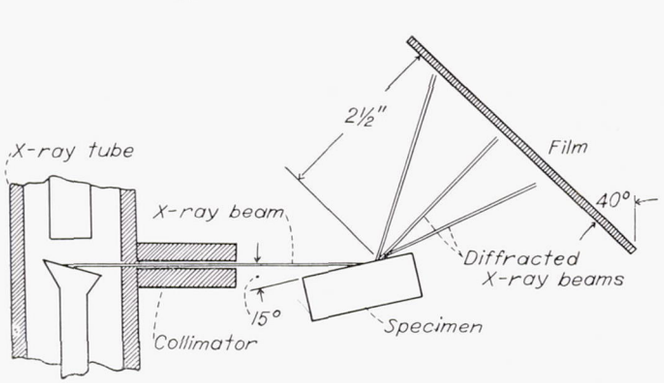


FIGURE 3.—Sectional schematic diagram of experimental setup for studying surfaces of polished samples.

In order to maintain a surface that was flat during the electrolytic metal removal, a special cell was designed as shown in figure 4. It consisted essentially of a 250-cubic-centimeter cylindrical container with a copper plate on the bottom as a cathode. This plate was connected to the source of current by a lead through a glass-metal seal. About one-half way up the cell, a watch glass containing a ⅝-inch hole was mounted horizontally. The metal sample acting as the anode was mounted ½ inch above the hole with the polished surface facing the hole. This hole acted to distribute the current evenly over the ⅞-inch-square surface at this distance, and thus a plane surface was maintained during metal removal. Water-cooling was used to prevent pitting associated with electrolyte temperatures above 100° C.

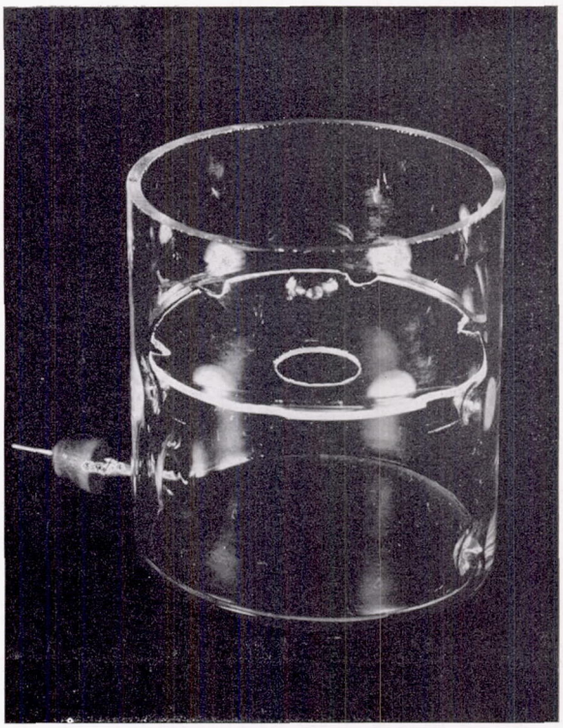


FIGURE 4.—Electrolytic cell for gross metal removal, X½.

The most satisfactory electrolyte was experimentally found to be a mixture of one-third concentrated hydrochloric acid (37 percent) and two-thirds glycerin. This mixture had the best current efficiency, approximately 0.0000625 inch of metal removed per ampere-minute at 8 amperes per square inch, without excessive pitting. A quantity of 200 cubic centimeters of this solution was sufficient for 6 to 10 samples. Pitting occurred when the metal ion concentration became too high. Phosphoric acid and glycerin combinations gave good polished surfaces, but had low current efficiencies. Sulfuric acid and glycerin mixtures caused passivation; mixtures of chromic acid or hydrofluoric acid with glycerin left the surface badly pitted.

(2) After the gross metal removal of step (1), the surface was given a high polish using undiluted Du Pont electropolishing solution for 5 minutes at 5 amperes per square inch. Metal removal in this step was negligible. The simple cell consisting of a beaker with a copper plate in the bottom was used for this step. No water-cooling was necessary. Of several other electrolytes tried for this step, only a mixture of 40 percent phosphoric acid and 60 percent glycerin was nearly as satisfactory as the Du Pont solution.

(3) After surface preparation, diffraction patterns were taken with the specimens either rotating or oscillating in the

X-ray beam. The grain size of the low-carbon N–155 specimens used was too large to present an effectively random distribution in the X-ray beam when the specimen was stationary. By moving the specimen under the beam during the time the diffraction pattern was being taken, a number of grains were presented to the beam in an effort to make the specimen approximately one of random grain orientation. In the case of line intensity measurements on a Norelco spectrometer, a specimen holder was designed and built which rotated the specimens at approximately 17 rps. Care was taken to insure that the plane of polish was perpendicular to the axis of spin. In the case of line width measurements, the specimens were oscillated $\pm 10°$ about an axis which was normal to the incoming X-ray beam, but parallel to the film. Finally, in making lattice-parameter measurements, the specimens were rotated at about 2 rps, with the axis of rotation parallel with, but offset from, the axis of the X-ray beam.

Diffraction-line peak-intensity studies.—The studies of diffraction-line peak intensity were confined to the [111] line of the austenite matrix, this line being the strongest line and within the range of the Norelco spectrometer. Copper $K\alpha_1\alpha_2$ radiation was used. Plots of the [111] line obtained with this spectrometer and an automatic recorder were measured graphically for peak height. Because the basic measurement needed was the line height of a given aged sample relative to unaged material, an unaged sample was run alternately with each aged sample.

Checks of the reproducibility of the [111]-line measurements were made by the following procedures:

(1) The unaged solution-treated sample, used as a standard of comparison, was taken twice through the surface-preparation step with, however, removal of only an additional 0.0025 inch of metal the second time. After taking the [111]-line height from the first surface, the X-ray tube and counter circuits were left on during the repolishing. The [111]-line measurements were immediately taken from the second surface and found to check within the accuracy of the spectrometer. This surface was carefully preserved and used as a standard for subsequent measurements on aged samples.

(2) The samples aged at 1200° and 1600° F were alternately measured for [111]-line peak intensity against the standard and repolished for a minimum of two and a maximum of six times. Between successive measurements 0.0025 inch of metal was removed. This was sufficient depth to bring up a new set of grains, since the average grain size of the samples used was approximately 0.001 inch.

(3) Despite the precautions, some scatter was still found in the measurements. In an effort to reduce this scatter, all the duplicate measurements on the samples aged at 1400° F were carried out on the same surface of each sample. These measurements were made on this surface with a 1-millimeter lateral shift in the holder between each run so that a new spot on the surface was covered by the X-ray beam each time. Two and usually three such measurements were made on each sample.

Diffraction-line width studies.—Line intensity studies on the [111] line of the low-carbon N–155 matrix with the Norelco spectrometer revealed no evidences of line broadening at any stage of the aging process. As a further search for broadening effects, a photographic back-reflection technique was chosen in order to take advantage of the increased resolving power in the back-reflection region. In addition, chromium radiation was used to eliminate, in part, fluorescence of the sample. Attention was centered on the highest-order line of the austenite matrix obtainable with the chromium radiation, the [220] line (at a diffraction angle, $\theta=65°$) resulting from the $K\alpha_1\alpha_2$ wave length. In order to record this line photographically, the samples were mounted at the center of a 20-centimeter circular camera with the irradiated area being oscillated $\pm 10°$ about an axis perpendicular to both the incoming X-ray beam and a diameter of the camera. Microphotometer recordings of the film showing the [220] $\alpha_1\alpha_2$ doublet were then made and the widths of the α_1 line determined at half peak intensity by graphical means. To correct for the presence of the α_2 line, the widths were actually measured as half widths on the side of the α_1 line away from the α_2 line, the division being a perpendicular through the apparent α_1 peak. While more rigorous methods are available to correct for the presence of the α_2 line, it is felt that the differences between them and the method actually used are of second order and that the accuracy of the rest of the technique did not warrant such corrections. Care was taken to make certain that the density range of the α_1-line recording lay within the linear-density and logarithmic-intensity range of the film. The microphotometer data were also corrected to read intensity against diffraction angle before broadening measurements were made. Correction for broadening due to all sources other than lattice strain was done by the method originally put forth by Warren (see reference 3) using unaged solution-treated low-carbon N–155 as a standard. It should be noted then that the line-broadening results are relative to the unaged material.

Lattice parameters.—Lattice parameters were measured with a Sachs and Weerts type camera using copper $K\alpha_1\alpha_2$ radiation. The samples were mounted with the prepared plane surface perpendicular to the incoming X-ray beam and rotated about an axis parallel with and slightly to one side of the axis of the X-ray beam. On the irradiated surface a light film of a mixture of mineral oil and chemically precipitated silver powder was placed. With the copper $K\alpha_1\alpha_2$ radiation used, two lines, among others, were photographically recorded, the [420] lines of the austenite matrix of low-carbon N–155 (at $\theta=75°$) and the [333] lines of the silver (at $\theta=78°$). From the measured spacing of the silver [333] lines and a lattice parameter of 4.0778 A for the silver, the camera-to-film distance was calculated for each exposure. With this calculated distance (which averaged approximately 10 cm) and measurement of the low-carbon N–155 [420]-line spacing, the lattice parameter for each of the various aged samples of solution-treated low-carbon N–155 was calculated. The absolute accuracy of these calculated parameters was not established, but the relative error was estimated to be ± 0.0005 A.

HARDNESS SURVEYS

Hardness surveys were made on the various samples with a Brinell machine using a 10-millimeter ball and a 3000-kilogram load. Two impressions were made on each sample, on planes which were originally transverse planes of the bar stock. Two perpendicular diameters of each impression were measured, and the resulting four readings were averaged and converted to the Brinell hardness number.

CREEP MEASUREMENTS

For the measurement of creep, 0.250-inch-diameter specimens were prepared with the axis of each specimen corresponding to the original axis of the bar stock. For the majority of tests the gage section was 1½ inches long terminated at each end with a ⅛-inch radius to the shoulder which in turn was ½ inch in diameter. Through the shoulders, 0.100-inch-diameter holes were diametrically drilled in which Chromel pins were driven. A modified Martens extensometer was attached to these pins for measurement of the extension under load. The least reading of this extensometer and associated telescope and scale was 10^{-5} inch.

For an additional check against the accuracy of extension measurements obtained in this manner, duplicate tests were run at the 60,000-psi stress level on samples aged at 1400° F and a different extensometer system was used. Here the samples had a gage length of 1¼ inches terminated at each end with a ¼-inch radius to a ⅜-inch-diameter shoulder threaded its entire length. Collars were then threaded onto these shoulders, down to the ¼-inch radii, and locked in place with setscrews. The extensometer system, in turn, was suspended from these collars with the use of pins mounted in the collars. Temperatures were controlled to ±5° F throughout the tests and the temperature differences along the gage length held to ±3° F. The furnaces used were electrical-resistance type split along a transverse section at the center for ease of control of the uniformity of the gage-length temperature. Load was applied to the specimen through a beam system with a mechanical advantage of 23.

In all tests the furnace was brought to the proper operating temperature before placing the specimen in it. The specimen was allowed to come to thermal equilibrium for an average period of 1½ hours during which time minor controller and temperature-uniformity adjustments were also made. At the expiration of the average period of 1½ hours, the specimen was loaded. It was felt that in this way, modification of the known initial structure of the specimens in the creep testing equipment prior to loading was held to a minimum. Thus, the short-time creep characteristics found, it is felt, truly represent the creep characteristics of the known initial structures without appreciable modification by time at the test temperature.

Two stresses were used in creep testing, 30,000 and 60,000 psi, and one temperature, 1200° F. The 30,000-psi stress was approximately the highest possible without excessive plastic deformation upon loading. The higher stress was used to determine how the stress level affected the conclusions concerning the effects of aging on creep resistance at 30,000 psi.

The creep tests were run for an average of 50 hours provided fracture had not occurred. These tests were restricted to 50 hours in order to obtain creep properties as characteristic as possible of the known initial structures and not the properties of the known initial structure plus modifications induced by time at the test temperature. At the end of 50 hours, all the tests covered herein had reached the so-called "second stage" of creep, with a reasonably steady creep rate, or had fractured. The creep rates reported are either these second-stage rates at 50 hours or the minimum rates occurring before fractures. It is obvious then that complete evaluation of decreasing secondary rates was not carried out.

RUPTURE TESTING

Rupture testing was carried out in three units. The tests under stresses above 60,000 psi were run in a hydraulic tensile machine equipped with a transversely split electric-resistance furnace. The load was held constant during the test to within ±1 percent with the rate of initial loading of the specimens approximately 50,000 psi per minute and comparable with the rate of loading of the more conventional rupture tests. Temperature control and uniformity over the gage length were the same as for the creep tests. Specimens for these tests were obtained by longitudinal quartering of the original ⅞-inch-square bar stock and using only those corners of the original bar which were uniformly fine-grained. Gage lengths 1⅜ inches long by 0.250 inch in diameter, terminated at the ends in ¼-inch radii to ⅜-inch threads, were machined in these quarter sections.

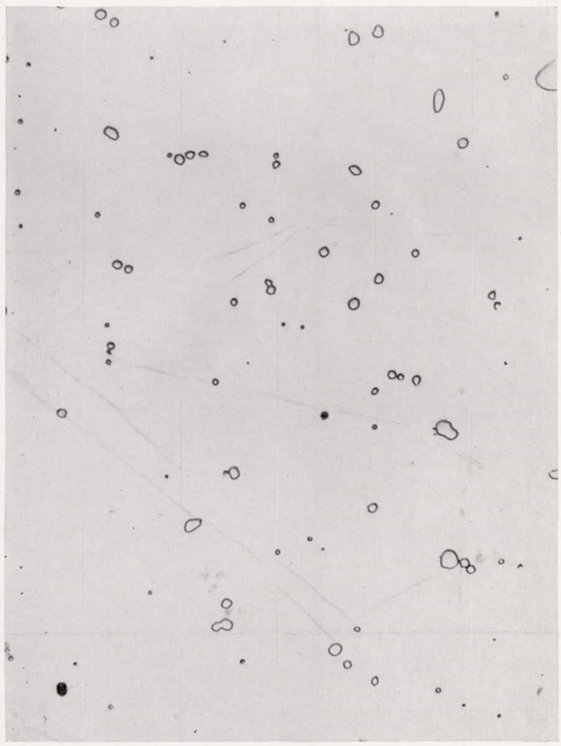
Tests at 60,000 psi were simply the creep tests carried to rupture. Tests at stresses less than 60,000 psi were run in conventional beam-loaded rupture units with one-piece electric furnaces and with temperature control and uniformity comparable with those of the other rupture and creep tests. Specimen form was the same as that used for the rupture tests in the hydraulic tensile machine.

RESULTS

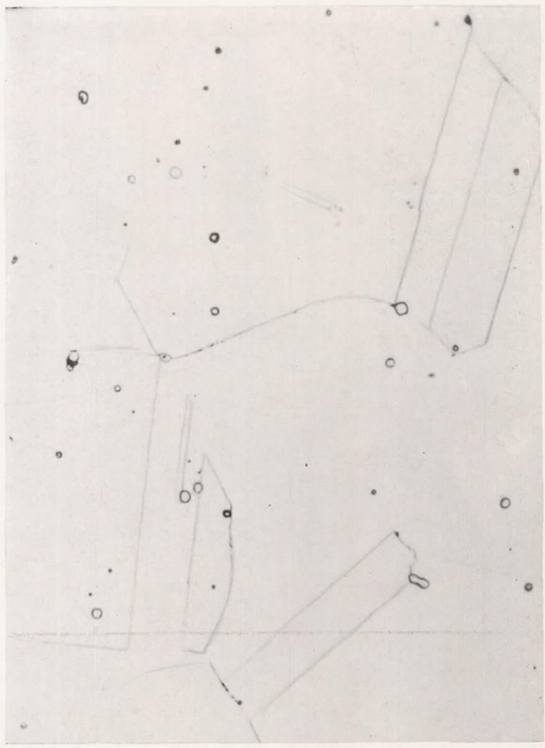
METALLOGRAPHIC EXAMINATION

Figures 5 to 9 show the micrographs taken of the aged samples and the following description summarizes the results:

(1) Aging at 1200° F resulted in little but the progressive development of a distinct grain boundary constituent which resisted etching. At aging periods up to 10 hours, the boundary constituent was incomplete in that it did not surround all the individual grains. At aging periods of 1000 hours, the boundary constituents completely surrounded the grains and had become an approximately 0.5-micron-wide band. After aging 1000 hours, slight precipitation was observable in the matrix near the grain boundaries. At 10,000 diameters, this precipitate did not appear to be a distinct phase with an interface but was surrounded by a concentration gradient as revealed by a sloping surface from the center of the precipitate particles to the matrix proper as a result of etching. As postulated by Nabarro (see reference 4) this could indicate that appreciable strains would exist around each such particle because of the probable difference in equilibrium lattice spacing between matrix and precipitate.



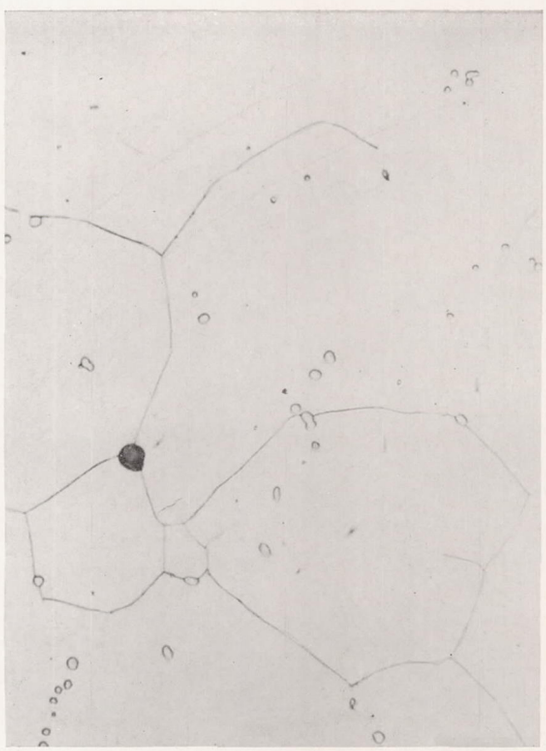
(*a*) Unaged.



(*b*) Aged 0.5 hour.



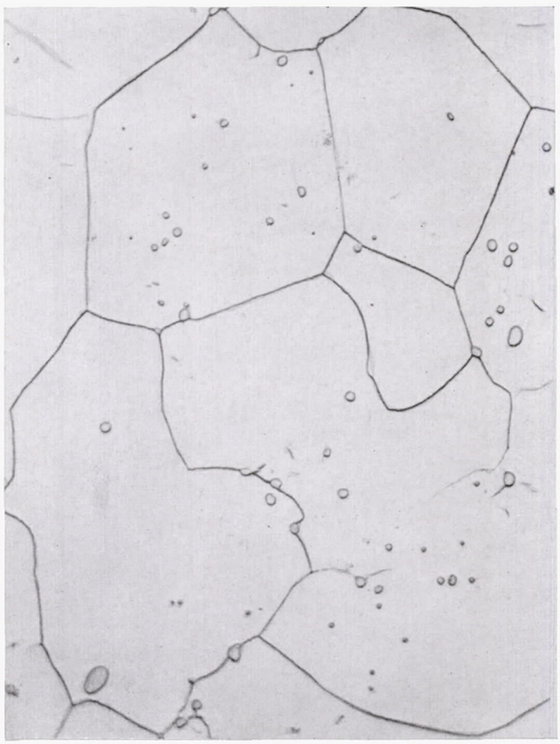
(*c*) Aged 1 hour.



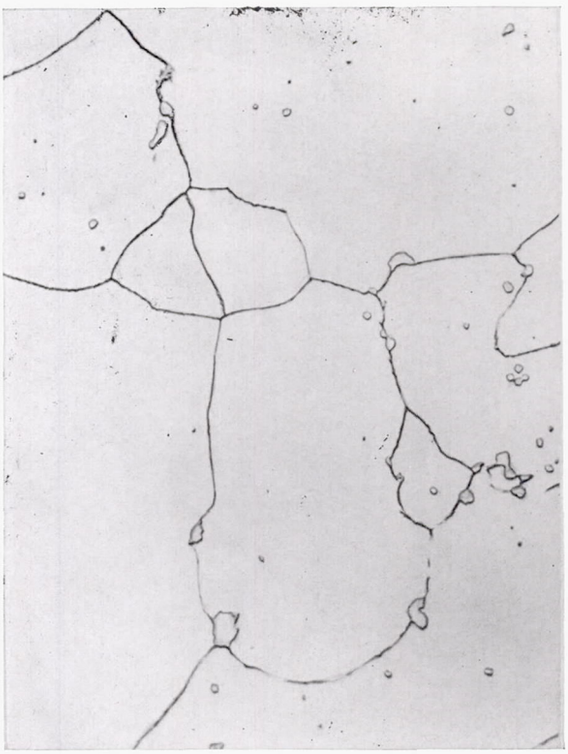
(*d*) Aged 3 hours.

FIGURE 5.—Effect of aging at 1200° F on microstructure of low-carbon N–155 alloy solution-treated 10 hours at 2200° F and water-quenched. Cross sections of bar, X1000. Electrolytically etched in 10 percent chromic acid.

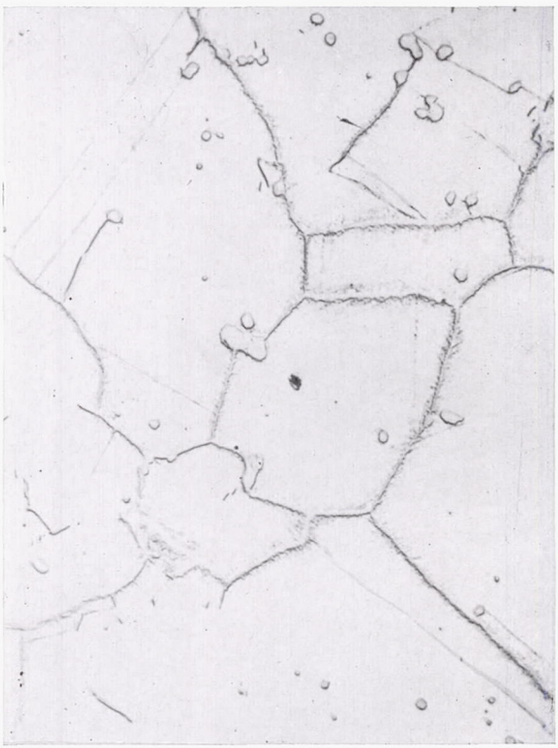
910097—51——2



(*e*) Aged 10 hours.



(*f*) Aged 30 hours.

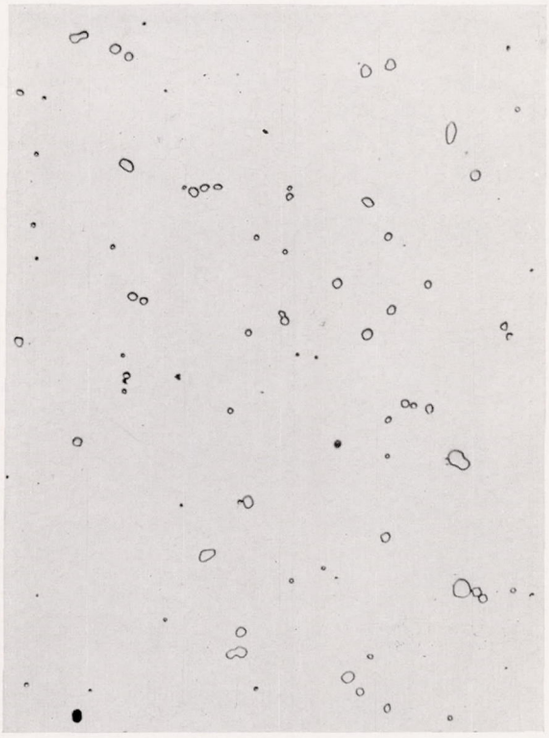


(*g*) Aged 100 hours.

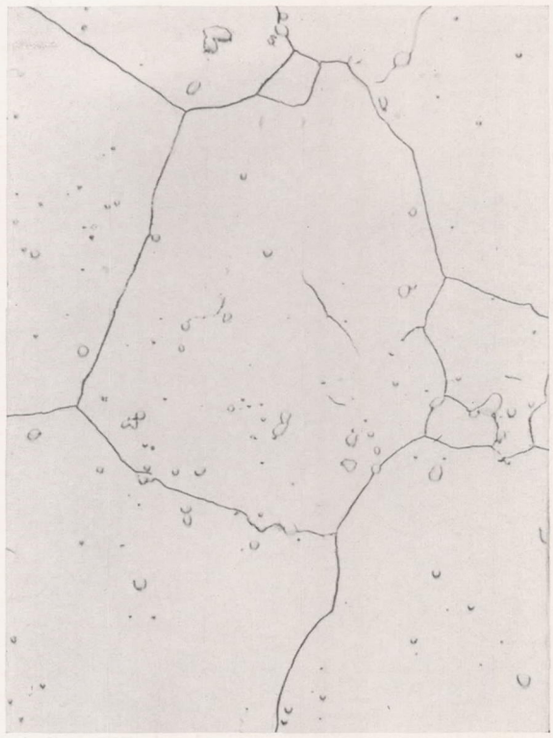


(*h*) Aged 1000 hours.

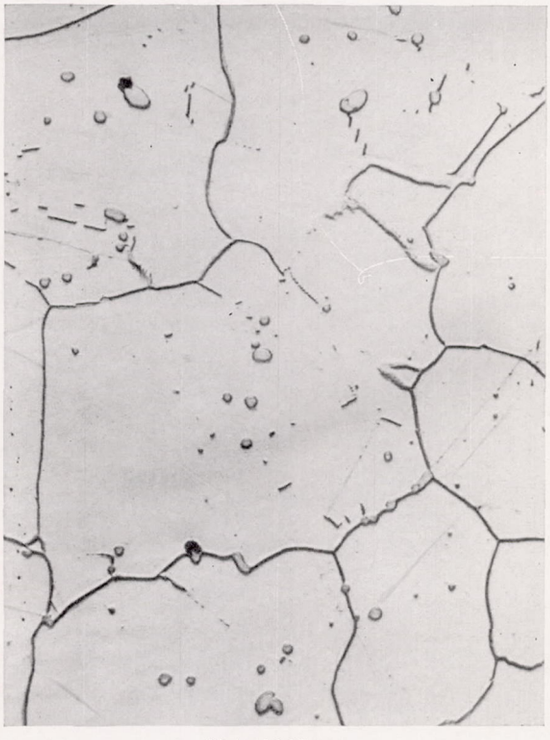
FIGURE 5.—Concluded.



(*a*) Unaged.



(*b*) Aged 1.0 hour.

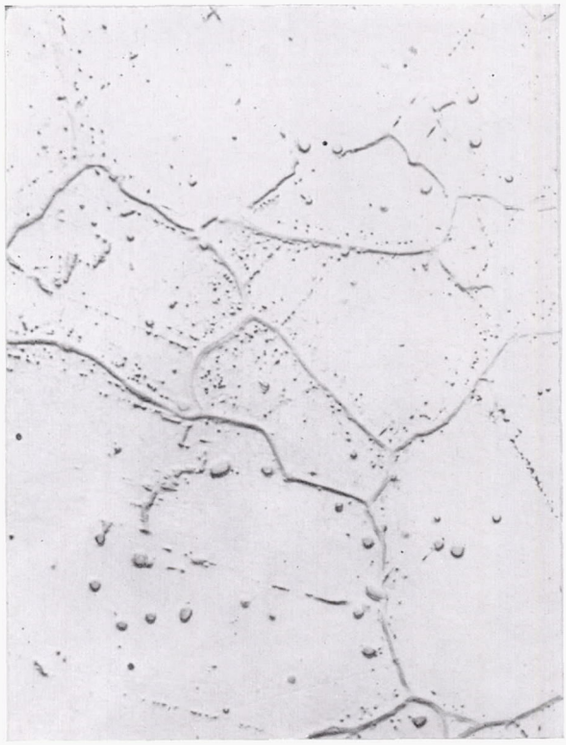


(*c*) Aged 3.0 hours.

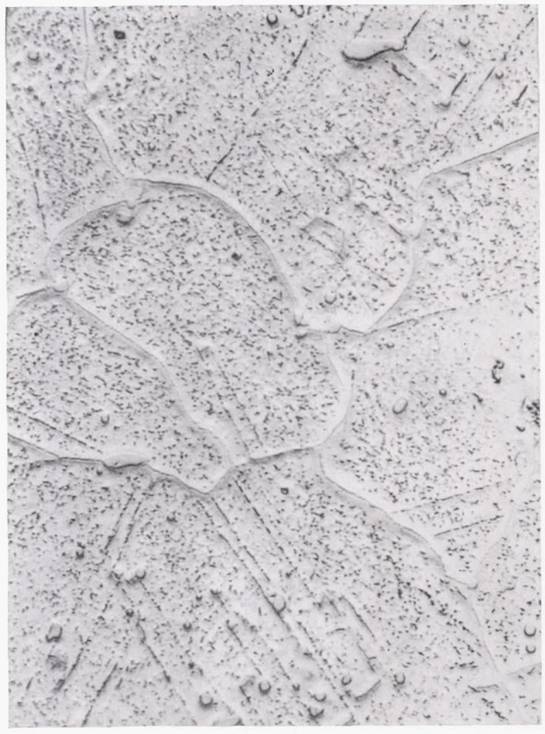


(*d*) Aged 10.0 hours.

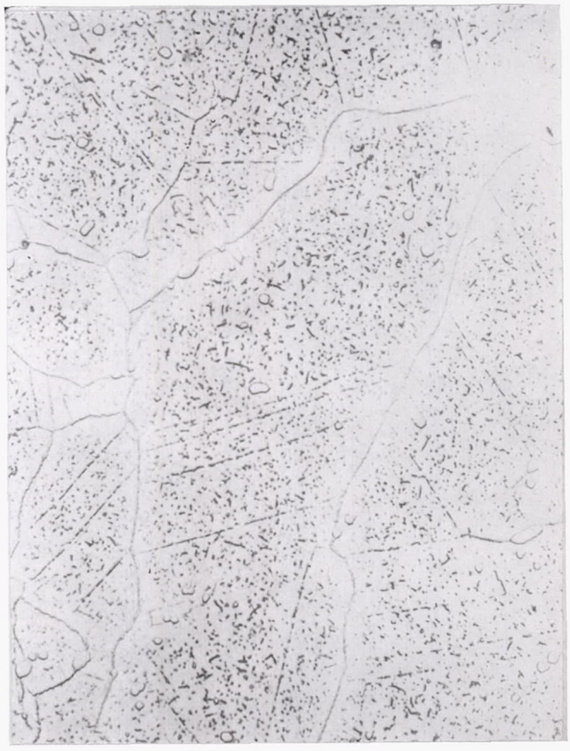
FIGURE 6.—Effect of aging at 1400° F on microstructure of low-carbon N–155 alloy solution-treated 10 hours at 2200° F and water-quenched. Cross section of bar, X1000. Electrolytically etched in 10 percent chromic acid.



(e) Aged 30 hours.



(f) Aged 100 hours.



(g) Aged 1000 hours.

FIGURE 6.—Concluded



(*a*) Unaged.



(*b*) Aged 1.0 hour.



(*c*) Aged 10 hours.

FIGURE 7.—Electron micrographs of replicas, X8500, prepared from low-carbon N–155 alloy solution-treated 10 hours at 2200° F, water-quenched, and aged at 1400° F.

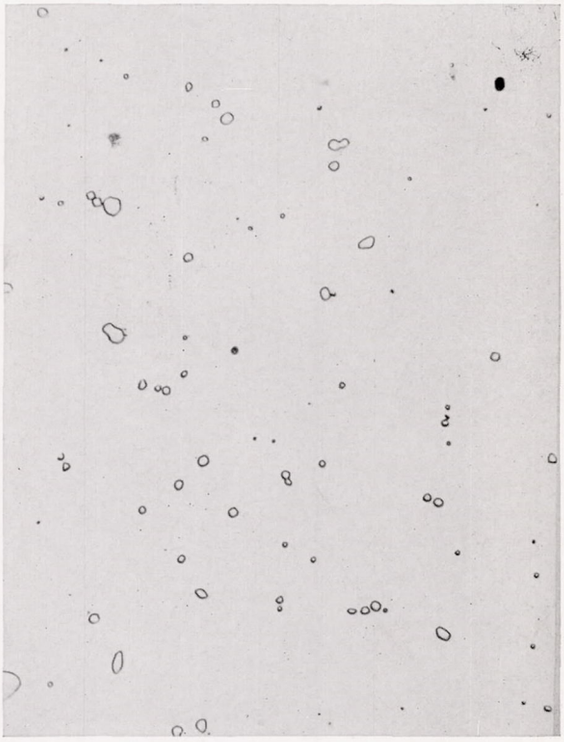


(*d*) Aged 100 hours.

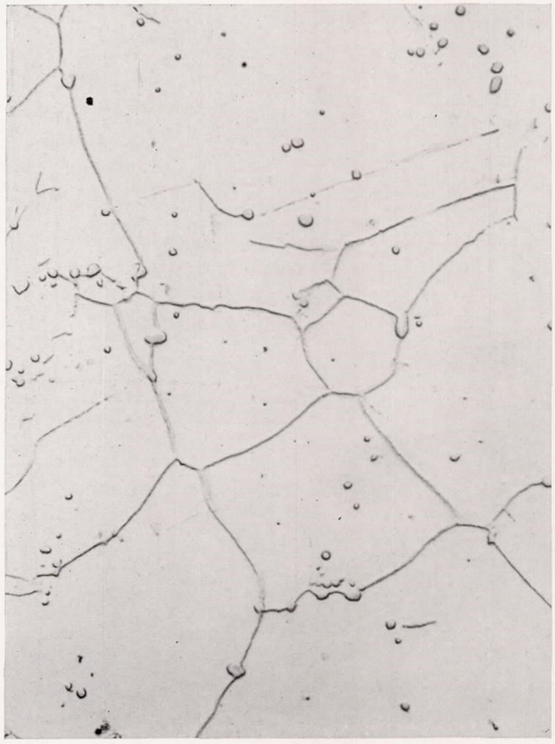


(*e*) Aged 1000 hours.

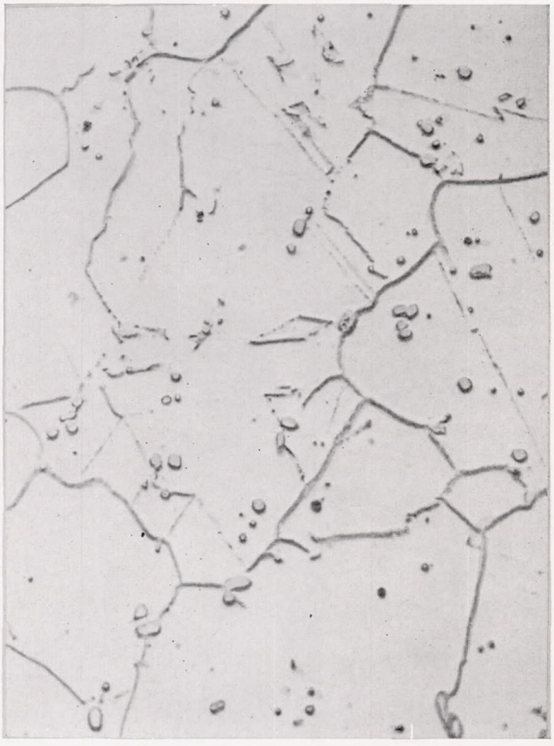
FIGURE 7.—Concluded.



(*a*) Unaged.



(*b*) Aged 0.5 hour.

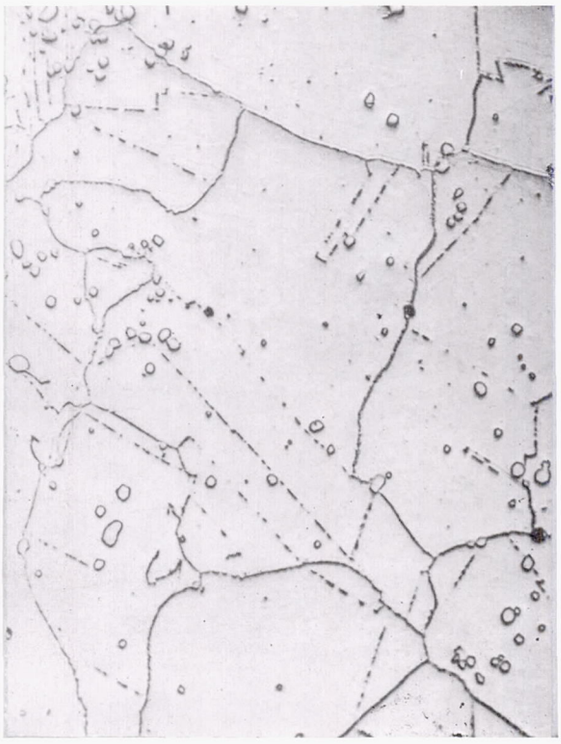


(*c*) Aged 1.0 hour.



(*d*) Aged 3.0 hours.

FIGURE 8.—Effect of aging at 1600° F on microstructure of low-carbon N–155 alloy solution-treated 10 hours at 2200° F and water-quenched. Cross section of bar, X1000. Electrolytically etched in 10 percent chromic acid.



(*e*) Aged 10 hours.



(*f*) Aged 100 hours.

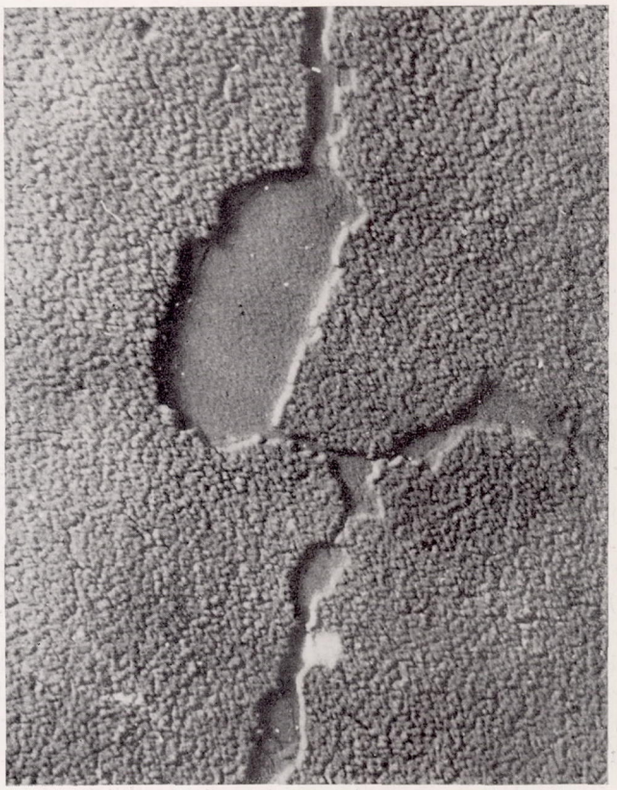


(*g*) Aged 1000 hours.

FIGURE 8.—Concluded.



(*a*) Aged 1.0 hour.



(*b*) Aged 10 hours.



(*c*) Aged 100 hours.



(*d*) Aged 1000 hours.

FIGURE 9.—*Electron micrographs of replicas, X8500, prepared from low-carbon N–155 alloy solution-treated 10 hours at 2200° F, water-quenched, and aged at 1600° F.*

(2) Aging at 1400° F, resulted first in the progressive development of a grain boundary phase. Initially only a concentration gradient was present at the boundary, as revealed by a sloping surface toward the grain boundary after etching. At 10 hours, the first separate boundary-phase particles appeared. At 100 hours, the boundary band was approximately 0.8 micron wide and changed little in character with further aging. In addition to the grain-boundary reaction, general matrix precipitation appeared after aging about 10 hours, first along the grain boundaries, and increased rapidly in number and size up to the longest aging period used, 1000 hours. The particles at first had concentration gradients surrounding them; however, for aging times of approximately over 100 hours, no appreciable concentration gradient appeared around the precipitate particles but rather a definite interface was present. Average size of the particles at 1000 hours was estimated visually to be 0.2 by 0.2 micron in the plane of polish and the particles were estimated to be spaced an average of 1 micron apart.

(3) Aging at 1600° F resulted in almost the same type of reactions as at 1400° F with the exception that they were accelerated. The boundary phase, for example, appeared after aging for 1 hour. The precipitate size at the end of 1000-hour aging was estimated to average 0.7 by 0.7 micron in the plane of polish and the particles were estimated to be spaced an average of 4 microns apart. Definite interfaces were present for each precipitate particle after aging times as short as 10 hours.

X-RAY STUDIES

Line intensity studies.—Figure 10 and table 1 show the results of line intensity studies on the 10-hour solution-treated material when aged at 1200°, 1400°, and 1600° F. Dehlinger (reference 5) and subsequent authors have considered the effects that short- and long-period lattice distortions have on diffraction lines. In essence the conclusions are that short-period disturbances (10^{-8} to 10^{-6} cm) result in reduction of line peak intensities without appreciable broadening and that long-period disturbances (10^{-5} to 10^{-4} cm) cause line broadening with, however, the integrated intensity remaining constant. Accordingly, the results of line peak-intensity studies shown in table 1 could be interpreted, in the absence of line-broadening data, as either short-period disturbances or long-period disturbances. If the latter were present, however, broadening should be the predominant effect.

The two minimums for the material aged at 1200° F in figure 10 lead to the possibility that two separate processes were observed at 1200° F. Aging at 1400° or 1600° F apparently resulted in only one process occurring at each temperature which decreased line peak intensity.

It will be noted that the scatter for the measurements on material aged at 1400° F was approximately the same as for the measurements on material aged at 1200° or 1600° F. Considering the two methods of measurement that were used, it is felt that the scatter was still due to unrandom grain distribution despite rotation of the samples. Before quantitative calculations can be made with such line intensity measurements, additional methods for alleviating unrandom grain distribution will have to be developed. Only qualitative conclusions are thus drawn from the intensity data in this report.

Matrix lattice-parameter measurements.—The measurement of lattice parameter as a function of aging time at a particular temperature can give direct evidence of whether the precipitate particles are still being nucleated, are growing by matrix depletion of the precipitate constituent atoms, or are growing by agglomeration. This usefulness of the parameter measurements is predicated upon the possibility of the average radii of the atoms making up the precipitate being somewhat larger or smaller than the average radii of the matrix atoms. If such is the case, then precipitation

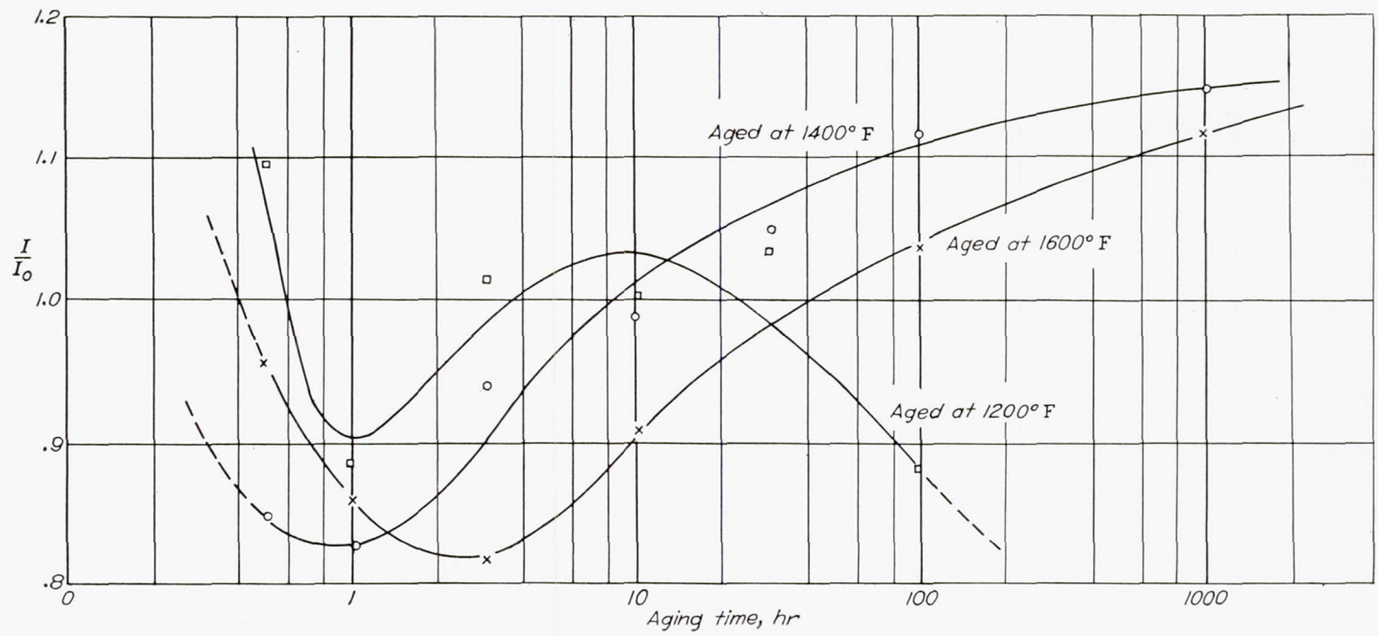


FIGURE 10.—Effect of aging on [111]-line intensity of low-carbon N-155 alloy solution-treated 10 hours at 2200° F and water-quenched. I, line peak intensity, indicated time; I_o, line peak intensity, unaged.

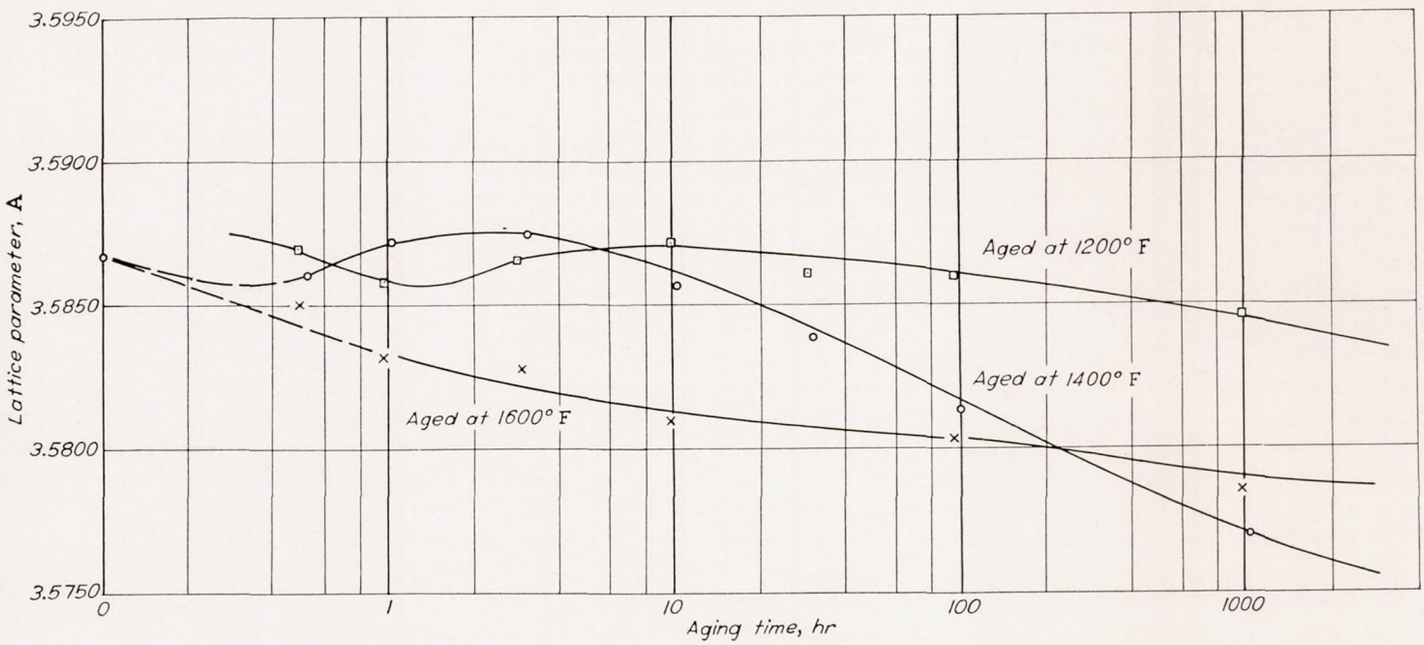


FIGURE 11.—Effect of aging on lattice parameter of low-carbon N–155 alloy solution-treated 10 hours at 2200° F and water-quenched.

by matrix depletion will result in a measurable decrease or increase in the lattice parameter. Nucleation can be ascertained if the lattice parameter remains constant for a period of time at a given temperature and then increases or decreases. Precipitate growth by agglomeration in turn can be noted when the parameter has reached a steady-state value after increasing or decreasing from the initial value and yet the precipitate particles continue to grow as evidenced by metallographic examination.

The results of parameter measurements on the solution-treated and aged low-carbon N–155 are shown in figure 11. In no case was the aging time sufficient to complete the precipitation reaction by matrix depletion, because the lattice parameters did not reach a steady-state value. For this reason, the relationship between the precipitate and matrix compositions and the temperature of aging was not definitely determined. It appears, however, that the precipitates obtained by aging at 1400° and 1600° F could have been slightly different in composition, since the curves for the matrix parameter approached steady-state values which were probably not quite the same. At the end of 1000 hours, aging at 1200° F had resulted in so little change in lattice parameter that the only conclusion was that the major volume fraction of the material was never out of the nucleation stage. In addition, a long nucleation period was shown by the lack of marked parameter change for aging up to approximately 100 hours at 1400° F followed by precipitate growth through matrix depletion. Only matrix depletion was found when aging was done at 1600° F.

Line width measurements.—Since Dehlinger (reference 5) had postulated that long-period lattice distortion (of the type which could be associated with each of the small precipitated particles revealed by the metallographic examination of samples after prolonged aging) would result in line broadening, it was decided to measure the line-broadening effects. The results of width measurements of the [111] line at $\theta=22°$, obtained from the Norelco spectrometer plots, showed little effect because of lack of resolving power. Figure 12 shows the line widths, expressed in radians, obtained from photometer plots of film recordings of the [220] line at $\theta=65°$. The increased resolution in the back-reflection region revealed that appreciable broadening appeared only after long-time aging at 1400° F and that a smaller degree of broadening occurred rather quickly when aging was done at 1600° F.

One further point is of importance here. The fact that the lattice parameter decreased with aging time makes it possible for a parameter distribution to be present as a result of concentration gradients being set up. Broadening of the diffraction lines will arise from this type of parameter distribution. Broadening could also arise from the elastic strains surrounding the precipitate particles, such elastic strains being due to a difference in atomic spacings in the two lattices. Thus, the broadening data presented here can be ascribed to two sources and unfortunately enough data are not at present on hand to separate the two effects.

HARDNESS MEASUREMENTS

The hardness survey was made to provide data for determining what internal condition gives high hardness. Figure 13 shows the results obtained on the solution-treated stock aged at 1200°, 1400°, and 1600° F. From figure 13, it can be seen that conventional aging behavior was apparently followed; that is, the higher the aging temperature, the sooner the approach to a maximum hardness—the maximum hardness, however, increasing in value with decreasing aging temperature. This was certainly true for aging at 1400° and 1600° F and probably true for aging at 1200° F.

CREEP PROPERTIES

The purpose of the creep and rupture testing carried out on solution-treated and aged low-carbon N–155 alloy was to

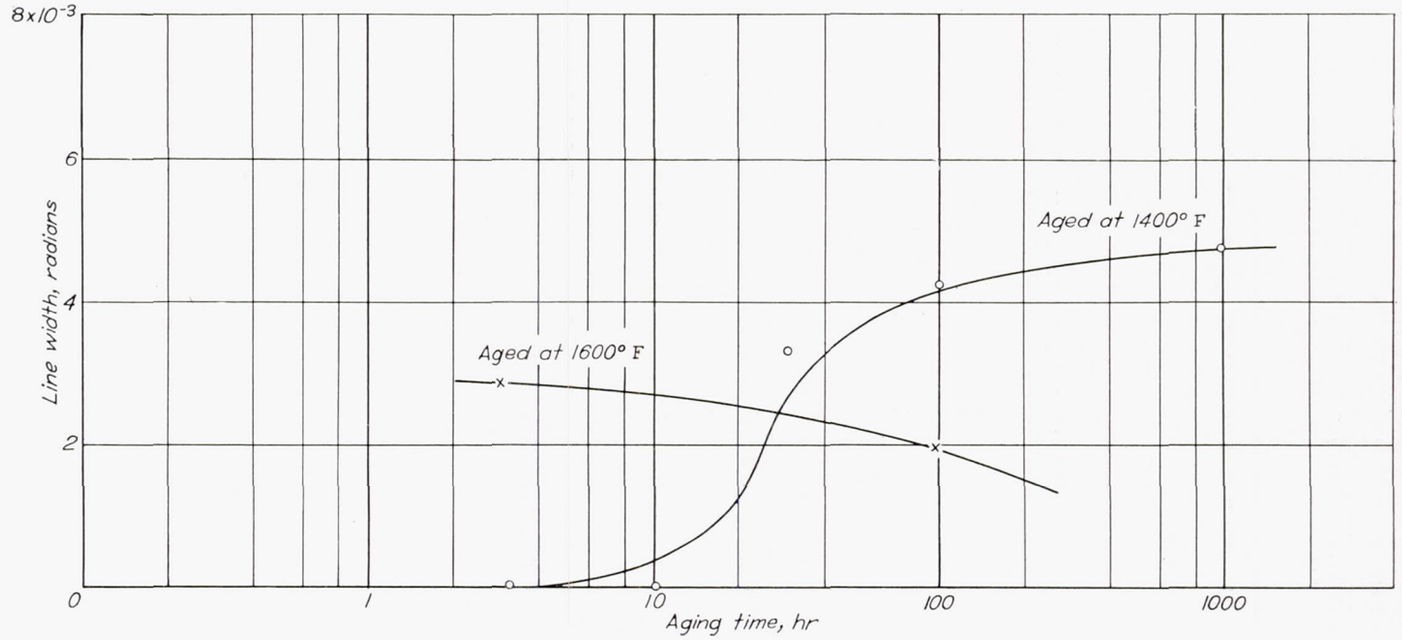


FIGURE 12.—Line width as a function of aging time at indicated temperatures for low-carbon N–155 alloy solution-treated 10 hours at 2200° F and water-quenched.

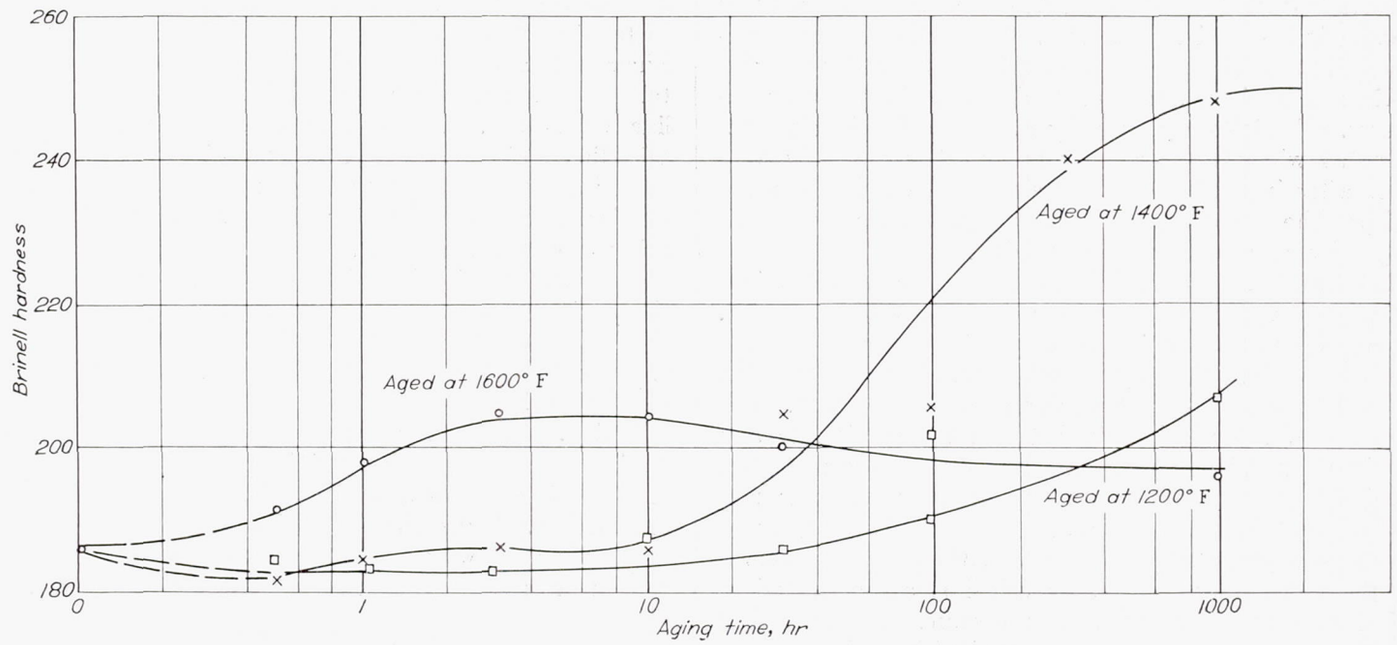


FIGURE 13.—Effect of aging on hardness of low-carbon N–155 alloy solution-treated 10 hours at 2200° F and water-quenched.

measure the mechanical behavior of samples used in the physical measurements discussed previously. Figures 14 and 15 and table 2 show the results of creep testing.

At the stress level of 30,000 psi (fig. 14), aging at 1600° F resulted in a rather uniform increase in the secondary creep rate. Aging at 1400° F for time periods up to approximately 10 hours resulted in little change in creep rate over the unaged material. For aging time periods over 10 hours, the creep rate increased rather rapidly to approach that for the material aged at 1600° F. From the two tests run after aging 100 and 1000 hours at 1200° F (100 hr being somewhat longer than the total period of creep testing) it appeared that aging at 1200° F had little effect on creep rate up to the longer aging period considered, 1000 hours, and then served only to reduce the creep resistance slightly.

Some ambiguity was present in determining the creep rate and aging relationship for aging at 1400° F. However, in view of the magnitude of experimental errors involved, it is felt that the curve shown is a reasonable compromise. In any event, the trend that long-time aging at 1400° or 1600° F tends to reduce markedly the creep resistance was clearly shown.

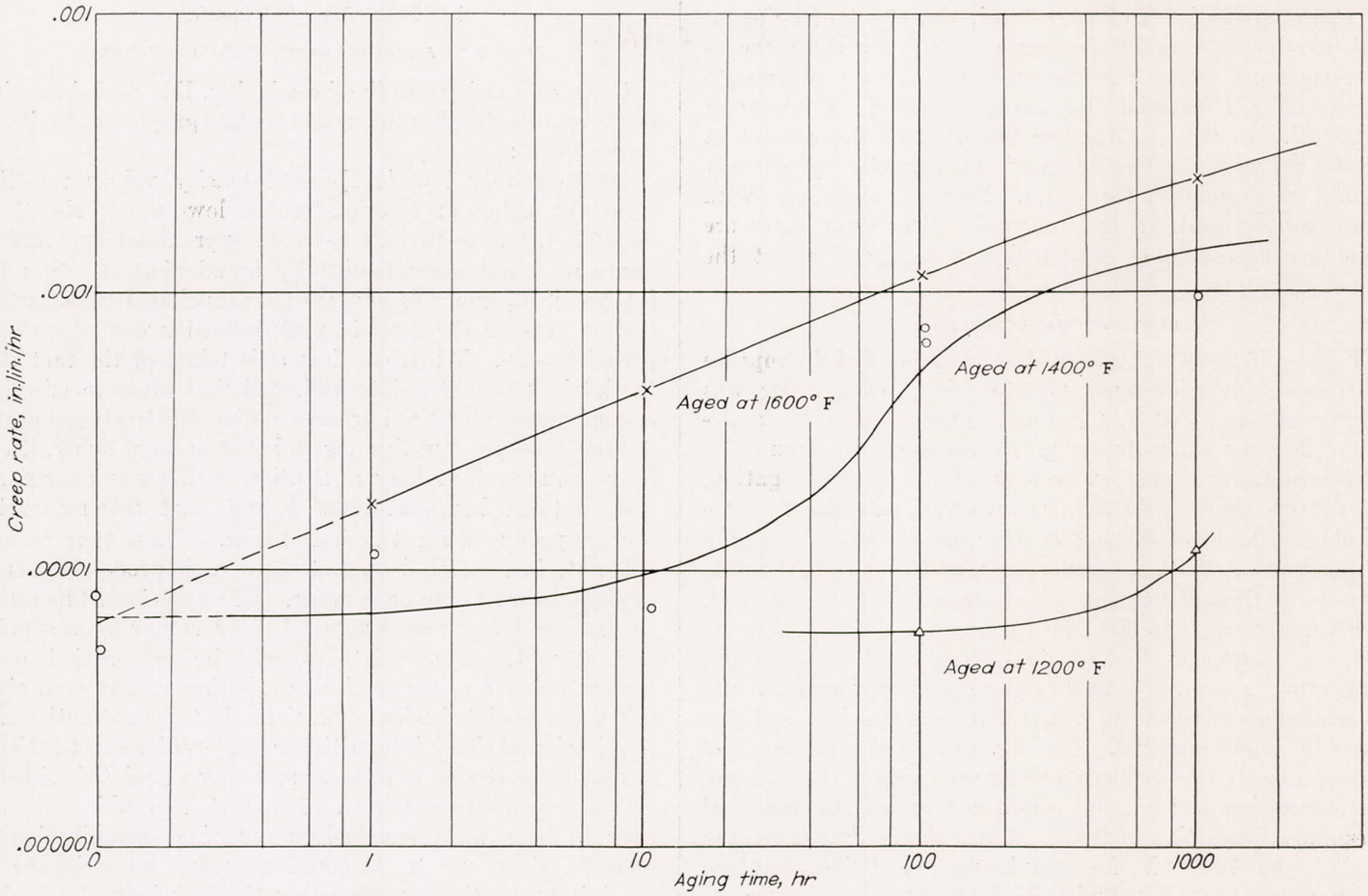


FIGURE 14.—Effect of aging on secondary creep rates at 30,000 psi and 1200° F of low-carbon N–155 alloy solution-treated 10 hours at 2200° F and water-quenched.

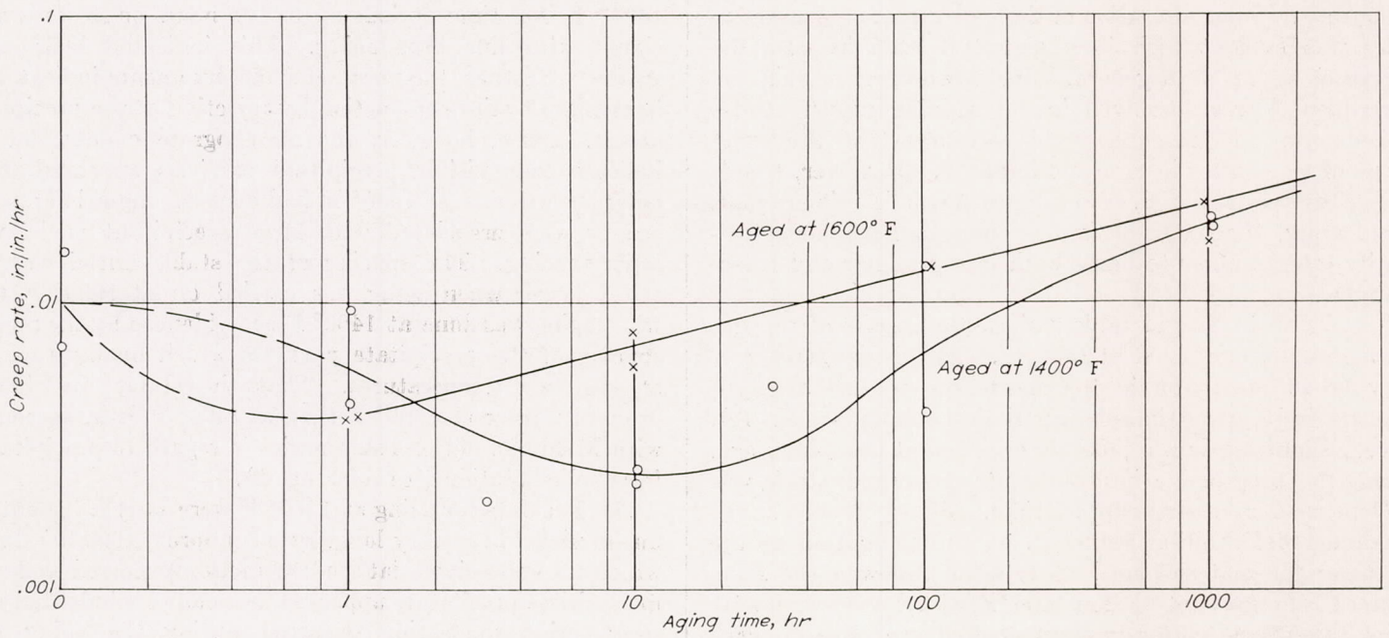


FIGURE 15.—Effect of aging on secondary creep rates at 60,000 psi and 1200° F of low-carbon N–155 alloy solution-treated 10 hours at 2200° F and water-quenched.

At the stress level of 60,000 psi, the effect of aging at either 1400° or 1600° F seemed qualitatively the same as at 30,000 psi except for the lower relative creep strength of the unaged material and the specimens aged 1 hour at 1400° F. It will be further noted that the results at 60,000 psi with the two types of extensometer agreed only within an average factor of 1.5. Previous experience with creep testing leads to the conclusion that creep rates are generally reproducible only within a factor of about the same magnitude.

RUPTURE CHARACTERISTICS

Figures 16 to 18 and table 3 show the results of the rupture testing on material aged at 1400° F. When aging was carried out at 1400° F, a gradual approach to a flat maximum in very short-time rupture strength occurred with increased aging time. Subject to additional investigation, for rupture times up to 10 hours, it appeared that no appreciable alteration of the initial structure occurred by virtue of reactions at the test temperature, and that the preceding result was thus due to the initial structure of the material. With increased time for rupture (greater than 10 hr), the main alteration in the relationship of rupture time and aging time appeared to be the marked improvement of the unaged and short-time-aged material in comparison with the long-time-aged material. (See fig. 16.) This improvement most probably was due to reactions occurring in the material during testing and will be considered under Discussion of Results. Inspection of figure 17 also shows that the aging periods at 1400° F for maximum short-time rupture strength were associated with the highest values of deformation prior to fracture. The initial deformation which occurred upon loading also increased slightly with increased aging time. Some alteration of these deformation characteristics was evident with increasing test time because the curves of figure 17 in general slope downward. Again the experimental error involved in determining rupture times and deformation obscured to a certain extent the exact shape of the curves in figures 16 and 17. However, trends were clearly established. From figure 18, it is evident that, upon aging, the mode of failure changed from being primarily intergranular to being both intergranular and transgranular.

Figures 19 to 21 and table 3 show the results of rupture testing on material aged at 1600° F. At this temperature a very broad maximum in the short-time rupture strength occurred with aging times longer than 0.5 hour (see fig. 19). A very slight maximum possibly occurred at the ½-hour age. Again the progressive improvement of unaged stock was evident with increasing rupture time. Figure 20 shows that maximum deformation values (i. e., the elongation at the fracture) for material aged at 1600° F followed the same pattern as for material aged at 1400° F, with, however, shorter aging times required for an equivalent effect (compare curve for ½-hr aging, fig. 20, with curve for 1-hr aging, fig. 16). Figure 21 shows that in no case were the predominately intergranular failures, found in the specimens aged a short time at 1400° F, observed in specimens aged at 1600° F even for as short a time as 0.5 hour.

DISCUSSION OF RESULTS

EFFECT OF AGING ON CRYSTALLINE STRUCTURE

Upon comparing the line-broadening, line peak-intensity, lattice-parameter, hardness, and metallographic data, it can be seen that:

(1) Relatively low [111]-line intensity values resulting from the aging of solution-treated low-carbon N–155 at 1400° F for time periods between approximately 0 and 30 hours were not accompanied by broadening of either the [111] or [220] line. It can thus be concluded that the distortion causing the drop in peak intensity was of a short-period nature. When cognizance is taken of the fact that the lattice-parameter data indicated that pronounced rejection of either interstitial or large-radius substitutional atoms did not take place until after 10 hours or so of aging, it can be postulated that only nucleation took place during the first 10 to 30 hours at 1400° F and that this nucleation process produced short-period strains. These time periods will not, in general, be exact since each process tends to overlap the next process to occur. The nuclei must be rather small since larger nuclei would have a rather large spacing and any strains associated would be long-period ones. Longer aging resulted in line-broadening strains and, since this was associated with appreciable lattice contraction due to rejection of either interstitial or large-radius substitutional atoms, these strains were most probably associated with the actual precipitate particles. The metallographic data appear to bear these conclusions out since examination at magnifications up to 10,000X revealed no evidence of precipitate particles until aging time periods at 1400° F were longer than 10 to 30 hours.

(2) Relatively low [111]-line intensities during aging at 1600° F for time periods up to 100 hours or so were associated with line broadening. This indicated long-period strains. Further, the parameter measurements indicated an immediate lattice contraction by rejection of the precipitant atoms. Since, however, the metallographic data did not indicate that visible precipitate particles appeared much before 100 hours at 1600° F had elapsed, these long-period strains were associated with large precipitant nuclei with large spacing. The spacing of the stable nuclei was certainly larger when aging was carried on at 1600° F than when aging was done at 1400° F as evidenced by the relative spacing of the precipitate particles which finally appeared at the two temperatures. That the stable nuclei were probably larger at 1600° F than at 1400° F is in agreement with Mehl and Jetter's summaries in regard to precipitation from solid solution (see reference 6).

(3) The data for aging at 1200° F were only fragmentary, but in view of the very long period (approx. 1000 hr) during which no appreciable lattice contraction occurred and very little visible precipitate appeared, one can conclude that only short-period nucleation occurred during the aging time studied. The changes in [111]-line intensity were then associated with the short-period strains of nucleation. The two separate minimums found could possibly be associated with, first, the matrix material in contact with the boundary and, second, the interior matrix nucleation.

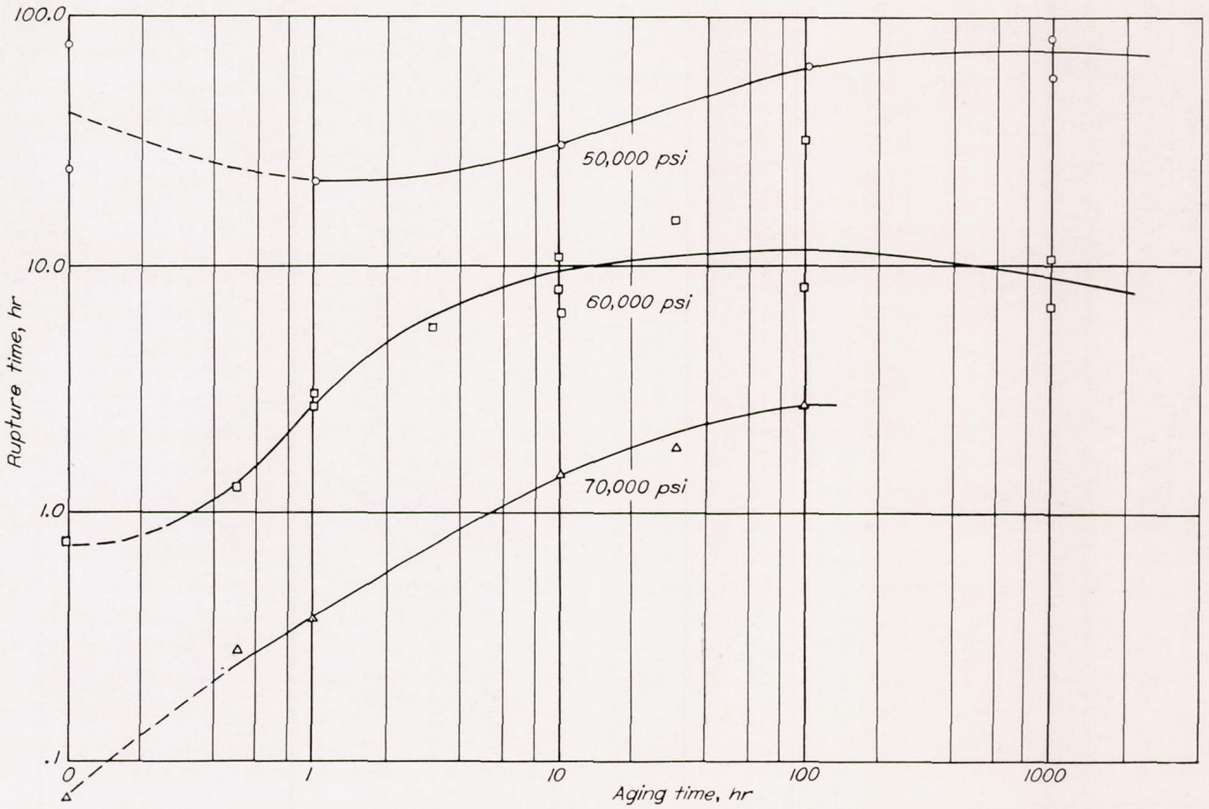


FIGURE 16.—Effect of aging at 1400° F on 1200° F rupture strength of low-carbon N–155 alloy solution-treated 10 hours at 2200° F and water-quenched.

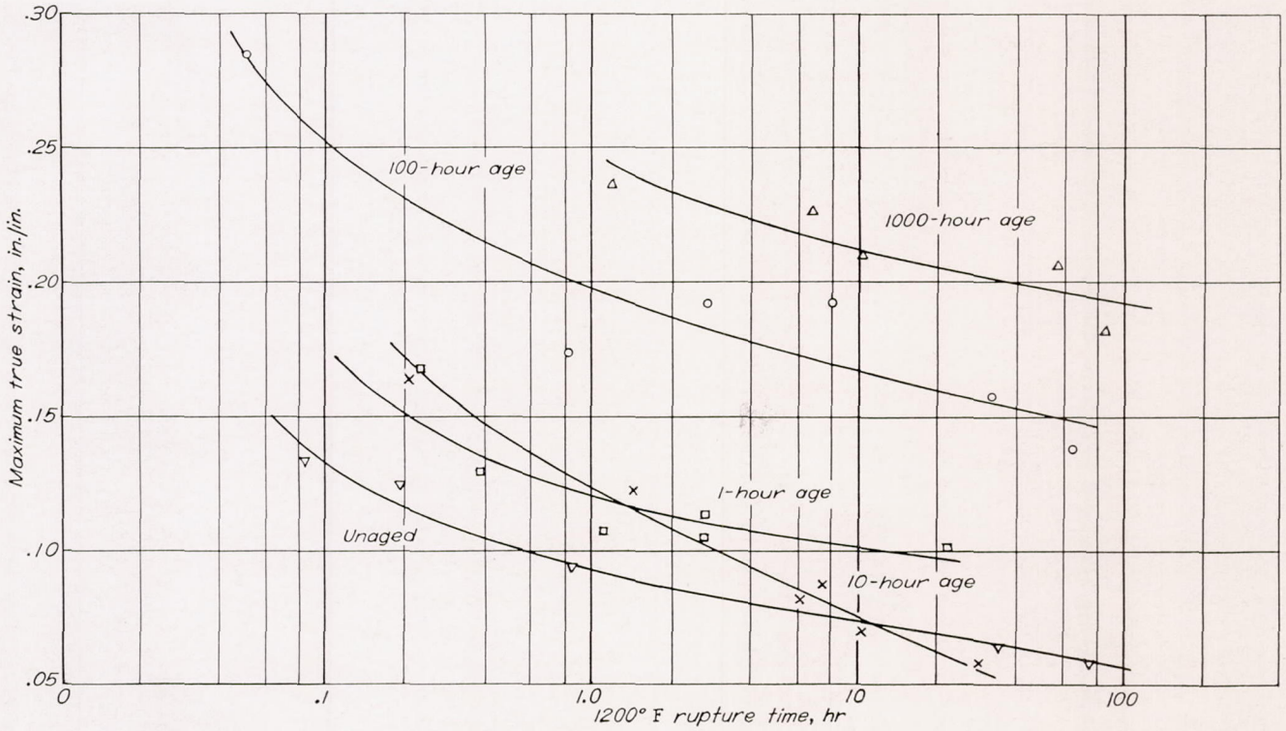
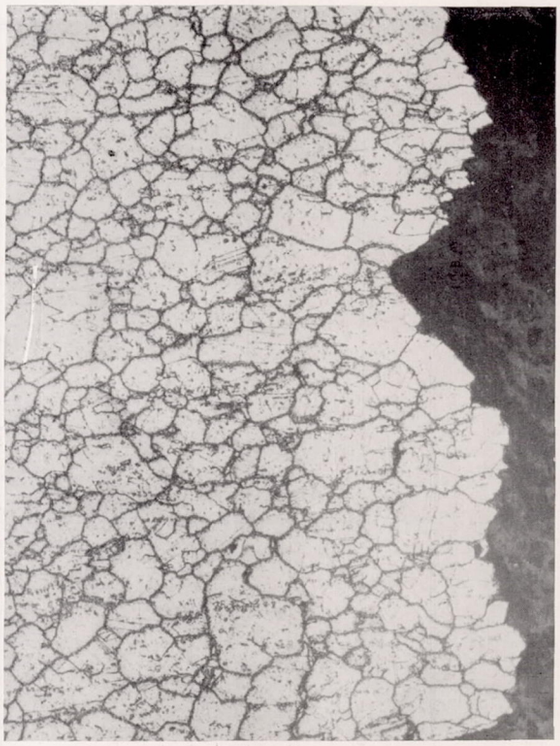


FIGURE 17.—Maximum true strain at rupture of low-carbon N–155 alloy aged at 1400° F, solution-treated 10 hours at 2200° F, and water-quenched.



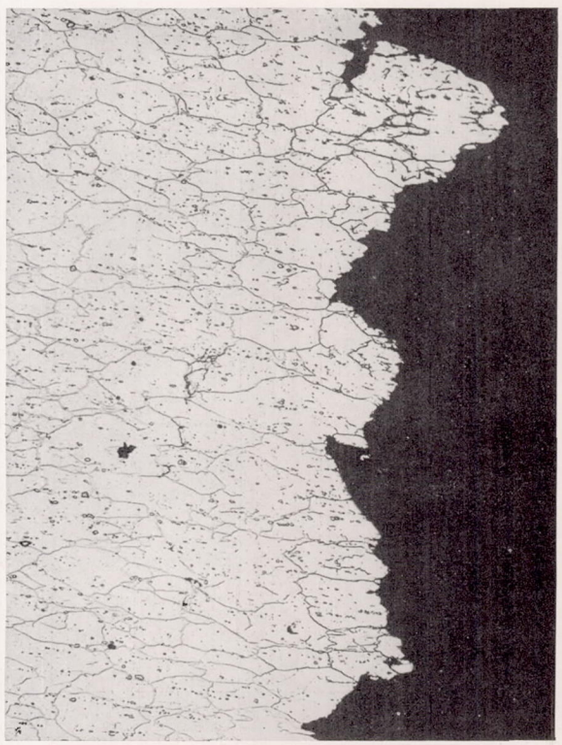
(*a*) Unaged; failed in 0.083 hour under a stress of 70,000 psi.



(*b*) Unaged; failed in 34 hours under a stress of 55,000 psi.



(*c*) Aged 1 hour; failed in 0.22 hour under a stress of 75,000 psi.



(*d*) Aged 100 hours; failed in 0.05 hour under a stress of 80,000 psi.

FIGURE 18.—Effect of aging at 1400° F on fracture characteristics at 1200° F of low-carbon N–155 alloy, X100, solution-treated 10 hours at 2200° F and water-quenched.

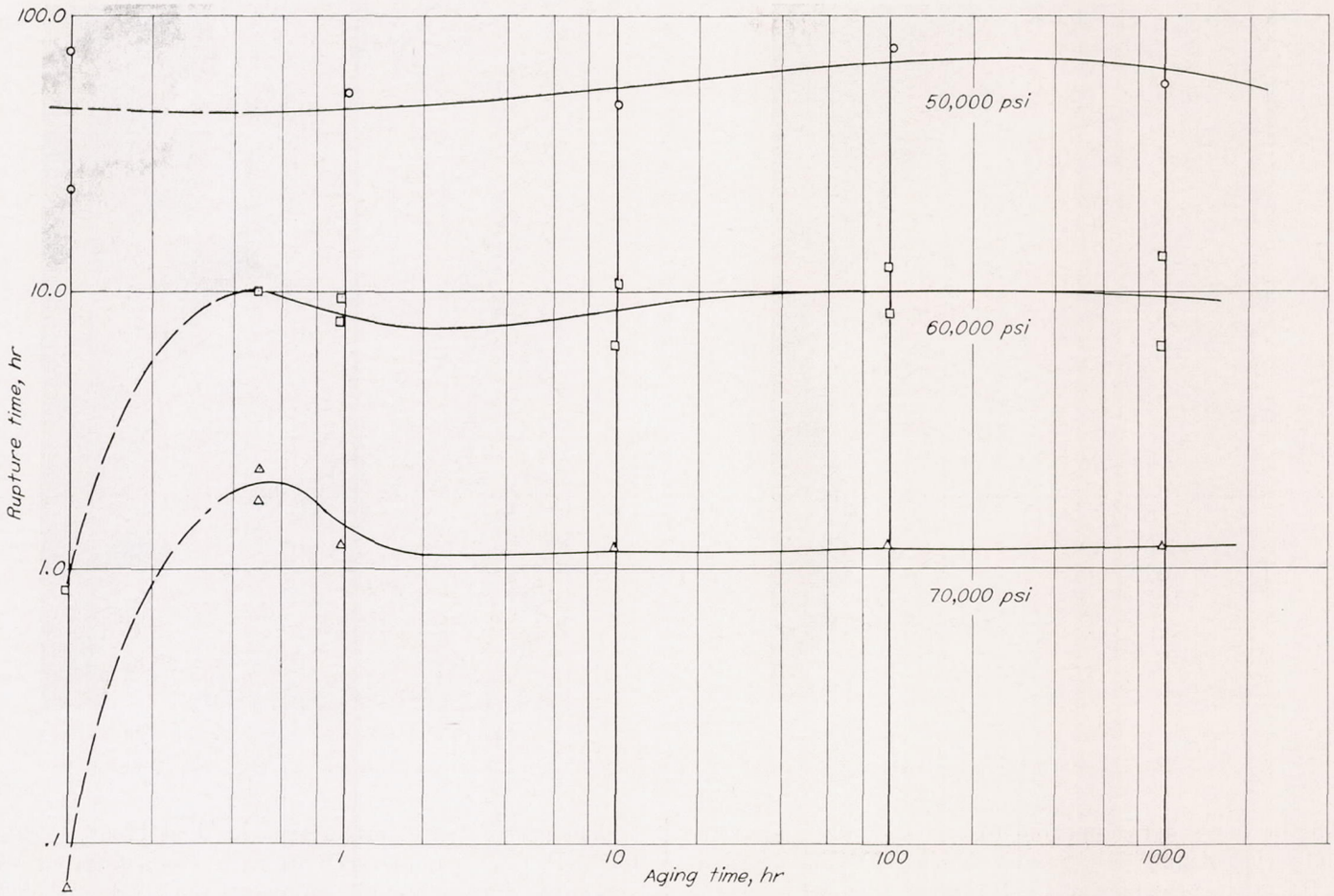


FIGURE 19.—Effect of aging at 1600° F on 1200° F rupture strength of low-carbon N–155 alloy solution-treated 10 hours at 2200° F and water-quenched.

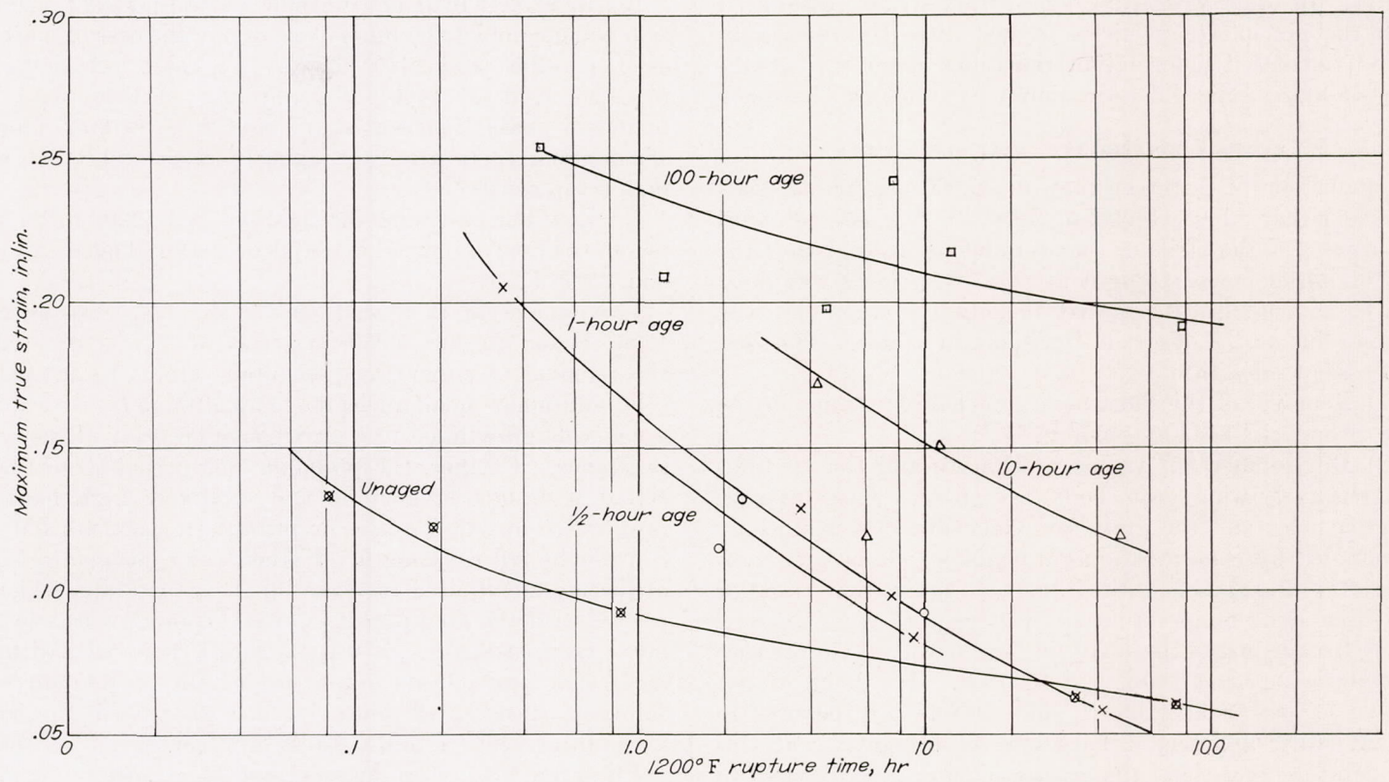
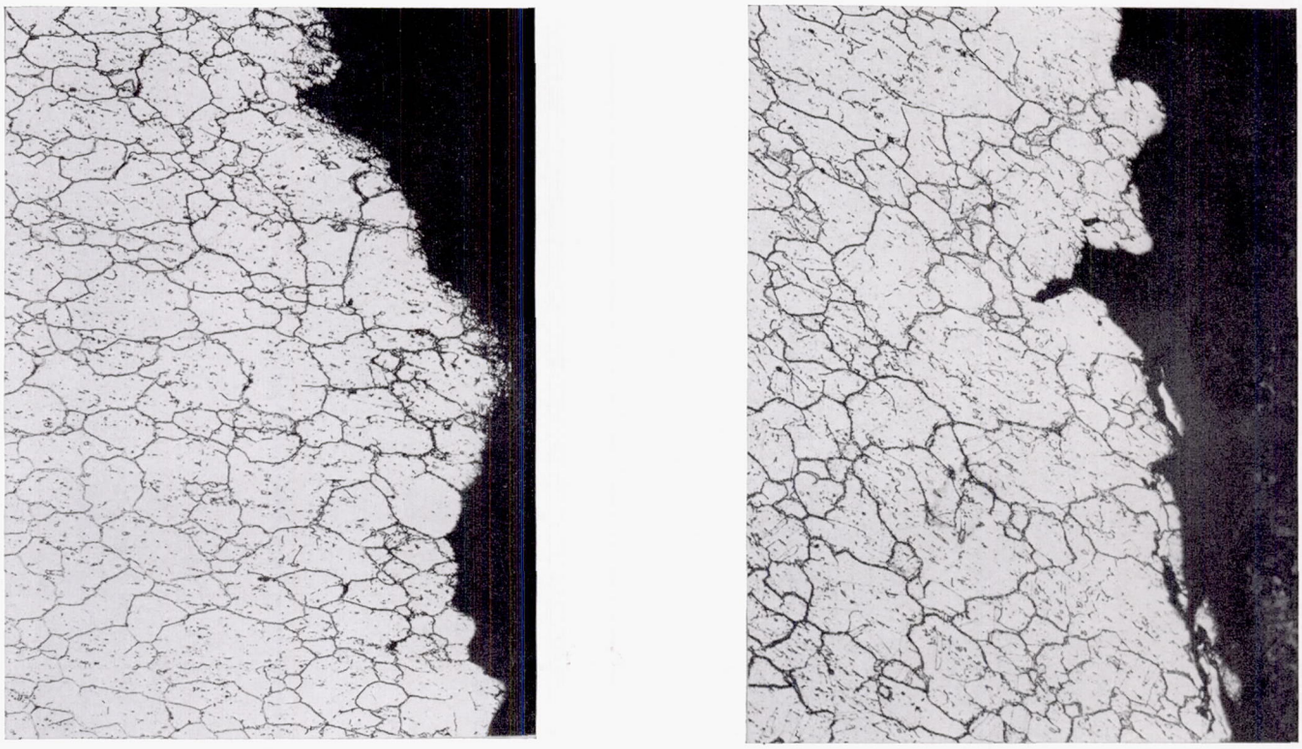


FIGURE 20.—Maximum true strain at rupture of low-carbon N–155 alloy aged at 1600° F, solution-treated 10 hours at 2200° F, and water-quenched.



(*a*) Aged 0.5 hour; failed in 1.81 hours under a stress of 70,000 psi.

(*b*) Aged 100 hours; failed in 1.25 hours under a stress of 70,000 psi.

FIGURE 21.—Effect of aging at 1600° F on fracture characteristics at 1200° F of low-carbon N-155 alloy, X100, solution-treated 10 hours at 2200° F and water-quenched.

The hardness data appeared to correlate quite generally with line broadening—the greater the degree of line broadening, the greater the hardness. Hardness, then, as far as the alloy studied is concerned, was associated with long-period strains. In other words, the long-period strains, associated with the precipitate particles formed after the nucleation period, increased deformation resistance under the conditions of large localized deformation present during a hardness test.

FACTORS CONTROLLING CREEP STRENGTH

Comparison of the creep rates at 30,000 psi for materials aged at either 1200°, 1400°, or 1600° F (see fig. 14) with the results of the structure measurements showed that the loss of initial creep strength at this stress level was most clearly associated with matrix depletion of the relatively large-radius or the interstitial precipitant atoms. This was also associated with:

(1) Removal of the short-period nucleation strains in the case of material aged at 1400° F.

(2) Development of visible precipitate and the continuous, relatively wide, grain boundary phase. These precipitant particles and the grain boundary phase were initially surrounded by concentration gradients which became progressively less steep with increased aging time (and/or increased aging temperature). (See figs. 5 to 9.)

(3) Broadening of the [220] line and hardening in the case of material aged at 1400° and 1600° F. The point is not known for aging at 1200° F since it was not possible to obtain either appreciable hardening or broadening at this temperature because of the excessive aging time required to reach high hardnesses.

Conversely, then, for materials aged at 1200°, 1400°, or 1600° F, retention of creep strength was associated with:

(1) As-solution-treated material or aged material still in the short-period nucleation state.

(2) Relatively little or no visible general matrix precipitation and incomplete boundary reaction in the case of material aged at 1200° and 1400° F. In all cases pertaining to material aged at 1400° F precipitate particles and the boundary phase, if present at all, had concentration gradients surrounding them after the aging periods associated with high creep resistance.

(3) Low hardness and the unbroadened [220] diffraction line in the case of unaged material or material aged at 1400° and 1200° F.

It would seem then that, as far as creep resistance at 1200° F and at the 30,000-psi stress level was concerned, the removal of either the precipitant atoms from random solid solution or small nuclei made up of them by subsequent precipitate growth led to a progressive lowering of the creep resistance. Further, the probable long-period strains associated with line broadening and relatively high hardness resulting from large nuclei or precipitate particles did not control the creep strength. Rather, the continued removal of the atoms required to make up the precipitate, which in turn caused the long-period internal strain, resulted in still lower creep strength. It was the strain associated with the individual precipitant atoms, while still in random solid solution or in small nuclei, which controlled the creep strength at 1200° F and a stress of 30,000 psi.

From figure 15 it can be seen that when considering creep resistance at 60,000 psi and 1200° F the effect of long-time

aging was qualitatively the same as at 30,000 psi, but that the material unaged and short-time aged at 1400° F had relatively less creep resistance than the same material at 30,000 psi. It thus appeared that, while long-time aging and concomitant matrix depletion of the precipitant atoms resulted in lowering of the creep strength, there was an optimum state of precipitation or nucleation and corresponding internal strain for an optimum creep resistance. However, an additional factor applied here. The relatively high stress of 60,000 psi resulted in fracture of all the creep specimens within a maximum of 32 hours. Figure 18 shows that the material unaged or short-time aged at 1400° F failed with general intergranular cracking. This formation of cracks resulted undoubtedly in greater creep rates than would be established with the same material with greater boundary strength. Hence, it was felt that the general effects of matrix depletion of the precipitant atoms observed at a lower stress level still apply but that the unaged and short-time-aged material has its creep resistance lowered, relatively speaking, at higher stresses by virtue of a weak grain boundary area.

The fact that the line-broadening strains, most probably associated with the individual precipitate particles, or large nuclei, which resulted in high hardness, did not have any effect on increasing creep resistance is quite surprising at first thought. However, since the short-period strains surrounding the individual precipitant atoms when in random or nearly random solid solution do give high creep resistance, it appears that the answer, as far as the alloy considered here is concerned, lies in the periodicity and size of the two types of strained regions. The atoms most likely to be the source of the short-period strains, in the solution-treated material, are tungsten, molybdenum, columbium, carbon, and nitrogen. The total atomic fraction of these atoms is 0.042, or one atom in 24. (See table 4.) In the absence of further data this can be interpreted to mean that one atom in 24 is the center of a strained region, the period of such strains being of the order of 6×10^{-7} centimeter. Since interatomic forces of solids in general extend over only a few atoms (see reference 7), the size of the strained regions might be assumed to be of the order of 1×10^{-7} centimeter. This leaves a mean strain-free-path of the order of 5×10^{-7} centimeter in the solution-treated material. In the aged material it seems plausible to assign the periodicity of the precipitate particles as the periodicity of the line-broadening strains. This spacing was of the order of 10^{-4} centimeter in the hardest sample prepared, that is, material aged 1000 hours at 1400° F.

It appears, unfortunately, that at present it is impossible to estimate closely the actual size, at any given aging time, of the strained areas associated with each of the precipitant particles or the average size of the precipitant-atom-free-paths. This is because enough is not yet known to separate the line broadening due to elastic strains from the line broadening due to concentration gradients in the matrix. However, it can be said that the mean precipitant-atom-free-path approached 10^{-4} centimeter as diffusion and precipitation approached completion. This path was more than two orders of magnitude greater than the original mean precipitant-atom-free-path.

The net result of aging, then, in solution-treated low-carbon N–155 alloy, was probably to replace a relatively short-period small-strain system containing a short mean strain-free-path (5×10^{-7} cm) with another larger-strain system of longer period and much longer mean strain-free-path (approaching 10^{-4} cm). Since creep as here considered is essentially a small-strain phenomenon, the few slip systems in operation had a considerably larger probability of running into a strained area per unit shear strain in unaged material than in aged material with any appreciable amount of precipitate, despite the large average strains in the latter system. This means lower creep resistance in the aged material. Hardness as commonly measured, however, is a large-strain phenomenon. The whole volume of the matrix is in a hardness test eventually filled with the many slip systems formed. The relatively large strains associated with the actual precipitate particles act very effectively to hinder the slip systems which eventually must form and try to pass through the large-strain areas during a hardness test. Thus, aged low-carbon N–155 is harder than unaged stock. A small-strain hardness test would probably give a much more accurate indication of the relative creep resistance of aged alloys of the low-carbon N–155 type.

Tungsten, molybdenum, and columbium can be considered sources of these short-period lattice strains since they are uniformly atoms of larger radii than those of the matrix and since aging in solution-treated low-carbon N–155 resulted in a decrease in lattice parameter, presumably by rejection from solution of these large-radius atoms. The matrix is assumed to be composed of iron, cobalt, nickel, and chromium, all atoms with approximately the same atomic radius (2.5 A). (See table 4.) Carbon and nitrogen present interstitially also act to expand the lattice and their removal through precipitation would make the lattice contract. Thus, these atoms must be considered along with tungsten, molybdenum, and columbium as sources of short-period strains while in random solid solution. The fact that solute atoms of considerably smaller or larger radius than those of the solvent introduce strain into the system when in solid solution is well-established generally, as witness the Hume-Rothery rules for solid-solution limitation (reference 8). To quote another source, Sir Laurence Bragg, "Most engineering alloys of importance are the ones deriving their strength, at least in part, from the modulation of the lattice due to the presence of foreign atoms of different size." [2] Further inspection of table 4 shows manganese and silicon to be atoms of smaller radius than the average radius for N–155; and these also could be sources of short-period strains. Manganese and silicon are probably in the lattice substitutionally and would tend to make its parameter smaller than normal and to make it increase with aging time if they were precipitating out. Preliminary chemical investigations indicated that only a phase or phases containing at most carbon, nitrogen, molybdenum, tungsten, columbium, chromium, and

[2] Lecture given at the University of Michigan, fall 1948.

iron were precipitating. Hence, it is believed that manganese and silicon play no part in the aging process, merely remaining in solution in the lattice throughout the aging process. It appears from these same preliminary chemical data that the carbon and nitrogen were partly in the form of an inert carbonitride of columbium in the solution-treated material. The fraction thus present was unknown, but even by disregarding entirely the carbon, nitrogen, and columbium content (which is most probably not correct) the conclusions as to the period of the strains involved are still warranted.

It appears that a logical way to increase the creep strength of low-carbon N–155 would be to add elements with either larger atomic radius than molybdenum, columbium, and tungsten or smaller atomic radius than carbon and nitrogen. Those suggested in table 5 are of the former type. Only boron, among elements of small atomic radius, appears promising at the moment. The usefulness of boron seems to be substantiated by the high creep strength of boron modifications of low-carbon N–155 recently investigated by the Union Carbide and Carbon Research Laboratories, Inc.

Table 6 lists elements which have atomic radii similar to molybdenum, tungsten, and columbium and which might be expected to act as substitutes. The elements suggested in these tables are not the only metallic elements with the desired atomic size but are thought to be the most promising. With the exception of aluminum and silver, all the proposed additions or substitutions are transition elements. Some evidence (see reference 9) is available which indicates that such transition elements have abnormally high binding energies. Aluminum and silver are considered only on the basis of having the desired apparent atomic size.

It is of course desirable that the materials suggested in tables 5 and 6 go readily into solution at some relatively high (solution-treating) temperature, and either stay in solution (or the nucleated state) or precipitate very slowly at the lower temperatures of service. It is possible that any or all of the proposed elements may show an increased tendency to come out of supersaturated solid solution and thus cause rapid loss of creep strength or show a wrong or poorer type of solubility-temperature characteristic. Other metallurgical characteristics (i. e., ductility) must necessarily be satisfied before such modifications could be considered satisfactory.

FACTORS CONTROLLING RUPTURE STRENGTH AND DUCTILITY

Inspection of figures 16 and 19 shows in general that aging at either 1400° or 1600° F resulted in a progressive increase in very short-time rupture strength. For a given increase in rupture strength, less aging time was required at 1600° F than at 1400° F. For somewhat longer rupture times, the relative increase in the rupture strength of the unaged material was quite striking. In fact, the solution-treated stock rapidly became equal in strength to the aged material at the increased rupture times. Previous experience has indicated that the rupture strength of the unaged material will actually exceed the rupture strength of the aged material when considering longer rupture times than were used in this investigation. Further, the maximum rupture times at each stress in figures 16 and 19 were approximately the same for aging at either 1400° or 1600° F. Examination of the other physical measurements shows that this general increase in very short-time rupture strength with increasing aging time was associated with:

(1) In the case of material aged at 1400° F, passage through the nucleation stage prior to precipitation as revealed by the line intensity studies.

(2) Removal of relatively large- or small-radius atoms through precipitate growth after nucleation as revealed by lattice-parameter measurements.

(3) Progressive formation of a rather wide, continuous band of a separate grain boundary phase and with the formation of the visible precipitate particles as revealed by micrographic examination.

(4) Hardening of the material through formation of strains which resulted in diffraction-line broadening in the case of aging at 1400° F and initial hardening and then progressive softening in the case of aging at 1600° F.

(5) Increased ductility of the specimens. One way to consider this effect is to express the maximum true axial strain at fracture based upon the initial and final cross-sectional areas at the fracture and the assumption of constancy of volume. Figures 17 and 20 present the results of these calculations. The effect of the decrease in cross-sectional area at the fracture with aging time was to increase the true stress during the duration of the test. In general, then, the rupture tests considered were not constant-stress tests, but rather tests with true stress increasing with time along some quantitatively unknown path in a time-stress coordinate system. It is known from the time-elongation curves for the tests at 60,000 psi that reduction of area was gradual and thus the true stress increased rather gradually throughout the test, the final value of course being greater for smaller final cross-sectional area. Inspection of the geometry of ruptured specimens showed that the cross section was reduced gradually along the axis toward the fracture. From this, it can be concluded that the degree of triaxiality of the stress system at the fracture was low, as considered in the calculations of Bridgman (see reference 10). Hence, the stress system can at least be considered uniaxial for the rupture tests covered herein. Lastly, figures 17 and 20 also show that the maximum true strain at fracture, or ductility, for any given class of specimen, decreased with increasing rupture time.

At the onset, the fact that ordinary rupture tests are not constant-stress tests makes outright analysis of the factors controlling rupture strength difficult. However, three factors stand out quite clearly:

First, figures 18 and 21 show that the relative initial weakness of the unaged materials was associated with weak grain boundary areas and consequent intergranular crack formation, especially on grain boundaries normal to the stress axis. Further inspection (see figs. 18 and 21) shows that this tendency for intergranular cracking was progressively removed with either increased aging time at 1400° or 1600° F prior to testing, or with decreased stress on the unaged material and thus increased time at the test temperature of 1200° F. This apparently was due to the formation of the grain boundary phase either prior to or during

testing (see figs. 6 to 9). Thus unaged material became stronger, relatively speaking, with increased rupture time and the aged material also became relatively stronger with increased prior aging time—more slowly, however, with prior aging time at 1400° F than for 1600° F aging since the boundary phase was formed more slowly at 1400° F. It is then quite interesting to conclude that the matrix- and boundary-phase binding was stronger than at least certain oriented matrix-matrix bindings.

Second, inspection of figures 16 and 19 shows that, once a definite almost continuous boundary phase was formed, the rupture strengths were roughly independent of aging temperature or aging time. This indicated that the initiation and propagation of the predominantly transgranular cracks were independent of the differences in structure arising from differences in aging at 1400° or 1600° F. Aside from minor maximums or minimums, which are probably just inside or outside the experimental errors involved in determining the rupture times, the differences in lattice depletion of the large-radius atoms and the differences in magnitude and time of occurrence of maximum hardening in specimens aged at different temperatures had little effect. This conclusion is based, however, in part upon the fact that the degree of elongation and cross-sectional area reduction, once the grain boundary phase was formed, was approximately the same for samples having the same rupture time as the result of aging at 1400° or 1600° F. Thus the degree of deformation was also constant and did not affect to a first approximation the fracturing characteristics of the two classes of aged materials differently. It is well-known, however, that, within limits, deformation in itself generally raises the resistance to rupture. (See reference 11.) Since this strain strengthening occurs in connection with increase in the true stress, evaluation of either of these two opposite effects is difficult along with evaluation of such things as the effect of progressive lattice depletion in general on resistance to crack propagation. Thus no further conclusions in regard to possible masked general structure factors arising with long-time aging at 1400° or 1600° F are drawn at this time.

Third, the plastic strain, before rupture failure occurred, increased markedly with long aging times at either 1400° or 1600° F. This of course is a direct result of the fact that the creep resistance decreased markedly with long aging times at either aging temperature and that the resistance to crack propagation on the other hand is at a maximum. Figures 17 and 20 also show, however, that the plastic strain before fracture decreased with increasing time for rupture. No obvious reason for this presented itself during the investigation covered herein.

LIMITATIONS OF RESULTS

This report is limited to the presentation of a method of determining the fundamental mechanisms by which processing, heat treatment, and chemical composition control the properties of alloys at high temperatures. A relatively limited amount of data for solution-treated and aged low-carbon N–155 alloy has been obtained and interpreted in terms of the proposed method. The resulting theories require extension and improvement from similar investigations on many alloys, as well as from more test conditions on low-carbon N–155 alloy. It is believed, however, that the approach to the problem is reasonably sound and that the limiting factors to a general theory of the metallurgical factors controlling high-temperature strength of alloys are the large volume of testing required and development of suitable experimental techniques.

In regard to low-carbon N–155 alloy, there are obviously numerous important aspects of the problem which have not been adequately covered by this report. Of primary importance is the fact that the structural measurements have not been correlated with long-time creep and rupture strengths at 1200° F or with any time period at other temperatures. Certain refinements in X-ray techniques seem desirable. Information is also needed regarding the effect of time and deformation during testing to assess the reliability of the assumption that such changes had little effect on known initial structure. And, finally, it would be especially desirable to know the exact composition of the precipitating phases. The amount of time required for development of suitable techniques and the volume of experimental work have been the limiting factors to date.

CONCLUSIONS

An experimental procedure is described which is believed suitable for establishing the fundamental mechanisms by which processing, heat treatment, and chemical composition control the properties of alloys at high temperatures. This method relates microstructures and X-ray diffraction characteristics, after various prior treatments, to creep and rupture test properties.

Application of this method to solution-treated and aged low-carbon N–155 alloy and correlation with the short-time creep and rupture characteristics at 1200° F indicated the following possible fundamental explanations for the effect of aging on the 1200° F properties:

1. Aging of solution-treated low-carbon N–155 resulted in progressive lowering of the initial (short-time) creep resistance through the removal from solid solution of large-radius or interstitial atoms by precipitation. No optimum precipitate dispersion or state occurred for optimum creep resistance; rather the alloy can be considered as obtaining its optimum creep strength through "modulation" of the lattice with the large or small precipitate atoms when they are in the random, or at most nucleated, distribution of the solution-treated state.

2. Short-time aging of solution-treated low-carbon N–155 apparently resulted in a marked increase in short-time rupture strengths over that for unaged material through the growth of a grain boundary phase, this phase acting to strengthen the boundary areas to eliminate intergranular cracking and consequent low resistance to crack propagation. Long-time aging resulted in little further change in short-time rupture strength, and longer-time testing at 1200° F was sufficient to develop a grain boundary phase in the unaged material and thus to raise its rupture strength to compare favorably with the strengths of prior-aged material.

3. Because the effect of aging in general was to lower the creep resistance and to raise the rupture strength, for

the time periods considered, aging resulted in a material which exhibited greater ductility before fracture.

It is indicated that alloys might be developed with strength comparable with that of N–155 by the use of other alloying elements, or that an alloy of the same general type with improved creep strength might be developed by replacing or supplementing the elements of large or small atomic radius present in low-carbon N–155. Elements of the same atomic radius as molybdenum, columbium, or tungsten, which could possibly act as substitutes or supplements, include aluminum, silver, and tantalum and elements of larger atomic radius suitable for additional alloying include zirconium, cerium, and titanium. Boron appears to be the only promising alloying element of small atomic radius not at present used in N–155.

It is emphasized that the foregoing explanations for the effect of aging on the properties of low-carbon N–155 alloy at 1200° F apply at present only to that alloy and are not to be taken as general. It is entirely possible that this alloy will prove to be an unusual one exhibiting behavior which is the exception to some general rule to be established as a result of further investigation on other alloys.

UNIVERSITY OF MICHIGAN,
ANN ARBOR, MICH., *January 18, 1949.*

APPENDIX

PROCESSING OF LOW-CARBON N–155 ⅞-INCH BROKEN-CORNER SQUARE BAR STOCK FROM HEAT A–1726

The Universal-Cyclops Steel Corp. reported the processing of the low-carbon N–155 bar stock to be as follows:

An ingot was hammer-cogged and then rolled to bar stock under the following conditions:

(1) Hammer-cogged to a 13-inch-square billet.
Furnace temperature, 2210° to 2220° F.
Three heats—Starting temperature on die, 2050° to 2070° F.
Finish temperature on die, 1830° to 1870° F.

(2) Hammer-cogged to a 10¾-inch-square billet.
Furnace temperature, 2200° to 2220° F.
Three heats—Starting temperature on die, 2050° to 2070° F.
Finish temperature on die, 1790° to 1800° F.

(3) Hammer-cogged to a 7-inch-square billet.
Furnace temperature, 2200° to 2220° F.
Three heats—Starting temperature on die, 2050° to 2070° F.
Finish temperature on die, 1790° to 1890° F.
Billets ground to remove surface defects.

(4) Hammer-cogged to a 4-inch-square billet.
Furnace temperature, 2190° to 2210° F.
Three heats—Starting temperature on die, 2040° to 2060° F.
Finish temperature on die, 1680° to 1880° F.
Billets ground to remove surface defects.

(5) Hammer-cogged to a 2-inch-square billet.
Furnace temperature, 2180° to 2210° F.
Three heats—Starting temperature on die, 2050° to 2065° F.
Finish temperature on die, 1730° to 1870° F.
Billets ground to remove surface defects.

(6) Rolled from a 2-inch-square billet to a ⅞-inch broken-corner square bar—one heat.
Furnace temperature, 2100° to 2110° F.
Bar temperature at start of rolling, 2050° to 2060° F.
Bar temperature at finish of rolling, 1910° F.

(7) Bars are numbered 1 through 56; bar 1 represents the extreme bottom of ingot and bar 56 the extreme top position.
All billets were kept in number sequence throughout all processing, so that ingot position of any bar can be determined by its number.

(8) All bars were cooled on the bed and no anneal or stress relief was applied after rolling.

REFERENCES

1. Freeman, J. W., Reynolds, E. E., Frey, D. N., and White, A. E.: A Study of Effects of Heat Treatment and Hot-Cold-Work on Properties of Low-Carbon N–155 Alloy. NACA TN 1867, 1949.
2. Thomassen, Lars, Williams, Robley C., and Wyckoff, Ralph W. G.: Surface Replicas for Electron Microscopy. Rev. Sci. Instr., vol. 16, no. 6, June 1945, pp. 155–156.
3. Warren, B. E., and Biscoe, J.: The Structure of Silica Glass by X–Ray Diffraction Studies. Jour. Am. Ceramic Soc., vol. 21, 1938, pp. 49–54.
4. Nabarro, F. R. N.: The Strains Produced by Precipitation in Alloys. Proc. Roy. Soc. (London), ser. A, vol. 175, no. 963, July 18, 1940, pp. 519–538.
5. Dehlinger, U.: Theory of Distorted Lattices. Zeitschr. Kristallogr., vol. 65, 1927, p. 615.
6. Mehl, R. F., and Jetter, L. K.: Symposium on the Age-Hardening of Metals. Am. Soc. Metals (Cleveland), 1940.
7. Seitz, Frederick: Modern Theory of Solids. McGraw-Hill Book Co., Inc., 1943, ch. 10.
8. Hume-Rothery, William: The Structure of Metals and Alloys. Third ed., Inst. of Metals (London), 1948.
9. Hume-Rothery, William: Atomic Theory for Students of Metallurgy. Inst. of Metals (London), 1948, p. 261.
10. Bridgman, P. W.: The Stress Distribution at the Neck of a Tension Specimen. Trans. Am. Soc. Metals, vol. 32, 1944, pp. 553–574.
11. Sachs, George: Effect of Strain on Fracture. Symposium on Fracturing of Metals, Am. Soc. Metals (Cleveland), 1948.
12. Lyman, Taylor (ed.): Metals Handbook. Am. Soc. Metals (Cleveland), 1948, p. 21.
13. Barrett, Charles S.: Structure of Metals. First ed., McGraw-Hill Book Co., Inc., 1943, p. 553.

TABLE 1

EFFECT OF AGING ON INTENSITY OF [111] LINE OF LOW-CARBON N–155 ALLOY SOLUTION-TREATED 10 HOURS AT 2200° F AND WATER-QUENCHED

Aging temperature (° F)	Aging time (hr)	Intensity, I/I_o [1]	Average intensity	Mean deviation from average
1200	0.5	1.102		
		1.049		
		1.075		
		1.169	1.099	±0.037
	1.0	.865		
		.935		
		.943		
		.822		
		.857	.885	±.044
	3.0	1.112		
		1.075		
		.975		
		.965		
		.955	1.016	±.06
	10.0	1.019		
		.967		
		1.041		
		1.000	1.007	±.025
	30.0	1.037		
		1.073		
		1.021		
		1.024	1.039	±.02
	1000.0	.854		
		.900		
		.872		
		.927	.888	±.023
1400	0.5	0.89		
		.82		
		.85	0.85	±0.02
	1.0	.83		
		.87		
		.80	.83	±.02
	3.0	.94		
		.94		
		.98	.95	±.02
	10.0	.99		
		.99	.99	0
	30.0	.97		
		1.05		
		1.12	1.05	±.05
	100.0	1.02		
		1.18		
		1.17	1.12	±.07
	1000.0	1.14		
		1.16	1.15	±.01
1600	0.5	0.91		
		1.01	0.96	±0.05
	1.0	.84		
		.88	.86	±.02
	3.0	.88		
		.72		
		.87	.82	±.07
	10.0	.92		
		.89		
		.93	.91	±.02
	100.0	1.01		
		1.05		
		1.06	1.04	±.02
	1000.0	1.21		
		1.02		
		1.14	1.12	±.07

[1] I peak intensity of sample aged as indicated.
I_o peak intensity of unaged sample.

TABLE 2

EFFECT OF AGING ON CREEP STRENGTH OF LOW-CARBON N–155 ALLOY SOLUTION-TREATED 10 HOURS AT 2200° F AND WATER-QUENCHED

Aging temperature (° F)	Aging time (hr)	Test temperature (° F)	Stress (psi)	Secondary creep rate (in./in./hr) [1]
1200	100.0	1200	30,000	0.000007
	1000.0	----------	30,000	.000012
1400	1.0	1200	30,000	0.000011
			60,000	.009
				.004
	3.0	----------	60,000	.002
	10.0	----------	30,000	.000007
			60,000	.0026
				.0025
	30.0	----------	60,000	.005
	100.0	----------	30,000	.000063
				.000070
			60,000	.013
				.004
	1000.0	----------	30,000	.000095
			60,000	.019
				.018
1600	1.0	1200	30,000	0.000017
			60,000	.0038
				.004
	10.0	----------	30,000	.000047
			60,000	.006
				.008
	100.0	----------	30,000	.000112
			60,000	.013
				.013
	1000.0	----------	30,000	.00025
			60,000	.021
				.017
Unaged	----------	1200	30,000	0.000005
				.000008
			60,000	.015
				.007

[1] The minimum observed rate at 60,000 psi or the rate between 40 and 50 hr after start of testing at 30,000 psi.

TABLE 3

RUPTURE CHARACTERISTICS AT 1200° F OF LOW-CARBON N–155 ALLOY SOLUTION-TREATED 10 HOURS AT 2200° F, WATER-QUENCHED, AND AGED AS INDICATED

Aging temperature (°F)	Aging time (hr)	Stress (psi)	Rupture time (hr)	Elongation (percent)	Reduction of area (percent)	Maximum true strain (in./in.) [1]
1400	0.5	70,000	0.27	23.8	22.6	0.126
		60,000	1.21	14.5	16.8	.091
	1.0	75,000	.22	26.1	28.2	.165
		70,000	.38	20.6	22.6	.126
		65,000	1.12	15.9	19.7	.109
		60,000	2.71	13.2	19.0	.105
			2.78	-------	20.5	.114
		50,000	22.00	11.6	18.0	.100
	3.0	75,000	.37	24.2	26.8	---------
		60,000	5.65	12.7	16.2	---------
	10.0	78,000	.21	27.7	27.5	.162
		70,000	1.45	22.0	21.8	.122
		60,000	7.80	19.1	16.2	.087
			10.05	13.0	13.1	.069
			6.25	-------	15.4	.084
		50,000	29.5	10.2	11.0	.058
	30.0	70,000	1.83	24.6	28.2	---------
		60,000	15.73	23.4	28.8	---------
	100.0	80,000	.05	30.6	43.7	.285
		75,000	.81	27.1	29.5	.174
		70,000	2.73	22.9	31.5	.194
		60,000	32.5	21.0	26.8	.157
			8.0	-------	32.2	.195
		50,000	63.0	23.5	24.5	.140
	1000.0	75,000	1.21	26.5	37.9	.240
		60,000	10.5	21.7	34.8	.213
			6.75	-------	36.6	.227
		50,000	82.75	27	30.7	.182
			59.5	27	34.2	.208
1600	0.5	70,000	2.25	19.8	23.4	0.131
			1.81	21.6	20.5	.113
		60,000	10.00	-------	16.8	.092
	1.0	75,000	.34	23.0	34.2	.207
		65,000	3.73	20.0	22.6	.128
		60,000	9.12	12.3	15.4	.083
			7.83	-------	17.6	.096
		50,000	41.0	4.5	10.7	.058
	10.0	65,000	4.38	26.1	29.5	.174
		60,000	10.83	22.5	26.2	.150
			6.25	-------	21.1	.120
		50,000	49.75	15.7	21.3	.120
	100.0	75,000	.45	35.4	39.8	.254
		70,000	1.25	29.4	34.2	.207
		65,000	4.57	27.5	33.2	.199
		60,000	12.50	30.8	35.6	.219
			8.0	-------	38.6	.242
		50,000	80	26.2	32.3	.192
	1000.0	73,000	.78	26.8	38.6	.243
		60,000	13.5	33.8	42.9	.279
			6.33	-------	44.6	.296
		50,000	57.5	45.0	30.0	.178
Unaged	------	70,000	0.083	19.9	23.4	0.131
		65,000	.192	16	21.8	.122
		60,000	.85	14	16.8	.092
		55,000	34.25	10.8	11.7	.062
		50,000	74.0	6.1	10.9	.058
			23.0	9.2	--------	---------

[1] $\epsilon_{max}=\log_e\frac{A_o}{A}$, at fracture section.

TABLE 4

ROOM-TEMPERATURE PHYSICAL CONSTANTS FOR LOW-CARBON N–155 ALLOY AND CONSTITUENTS

Metal	Crystallographic system	Unit cell size (kX)	Closest approach of atoms (kX)	Atomic fraction in low-carbon N–155 [a]
[b] Iron	Body-centered cubic	2.8606	2.476	[c] 0.322
[b] Chromium	do	2.8787	2.493	.233
[b] Nickel	Face-centered cubic	3.5167	2.486	.185
[d] Cobalt	Close-packed hexagonal	2.502, 4.066	2.494	.192
	Face-centered cubic	2.540	2.502	
[b] Manganese	Cubic (complex)	8.894	2.240	.0171
[b] Silicon	Diamond cubic	5.4173	2.346	.0085
[b] Carbon	Hexagonal	2.4564,6.6906	1.420	.00618
[b] Nitrogen	------	------	------	.00532
[b] Tungsten	Body-centered cubic	3.1585	2.734	.00813
[b] Columbium	do	3.2941	2.853	.00521
[b] Molybdenum	do	3.140	2.720	.0174
Low-carbon N–155	Face-centered cubic	[e] 3.580	2.54	1.000

[a] Converted from data reported by manufacturer.
[b] Reference 12.
[c] By difference.
[d] Reference 13.
[e] Solution-treated.

TABLE 5

ELEMENTS OF ATOMIC RADIUS OVER 2.8 A FOR POSSIBLE USE IN LOW-CARBON N–155 ALLOY

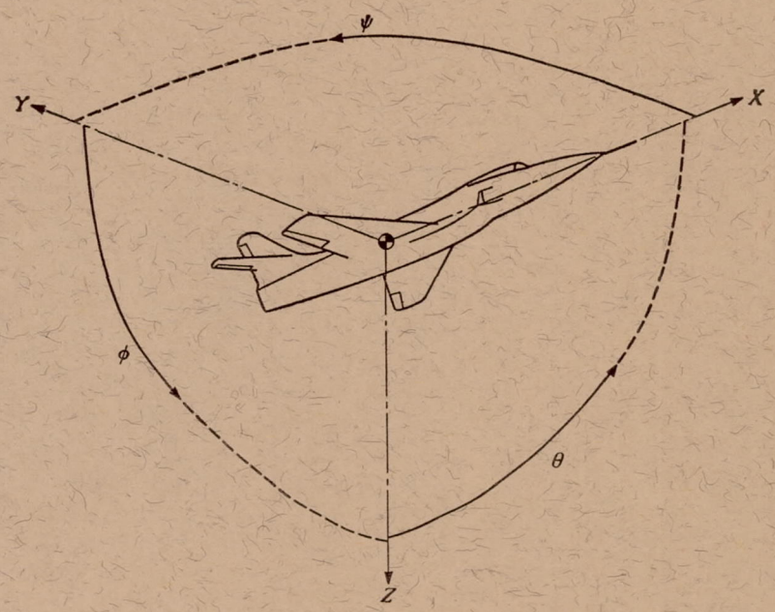
Element	Crystallographic system	Unit cell size (A)	Closest approach of atoms (A)
Cerium	Face-centered cubic	5.143	3.64
Zirconium	Close-packed hexagonal	3.223, 5.123	3.16
Titanium	do	2.953, 4.729	2.91

TABLE 6

ELEMENTS WITH AN ATOMIC RADIUS OF APPROXIMATELY 2.8 A FOR SUBSTITUTION FOR TUNGSTEN, MOLYBDENUM, OR COLUMBIUM IN LOW-CARBON N–155 ALLOY

Element	Crystallographic system	Unit cell size (A)	Closest approach of atoms (A)
Aluminum	Face-centered cubic	4.0408	2.856
Silver	do	4.2774	2.880
Tantalum	Body-centered cubic	3.2959	2.850

U. S. GOVERNMENT PRINTING OFFICE: 1951



Positive directions of axes and angles (forces and moments) are shown by arrows

Axis		Force (parallel to axis) symbol	Moment about axis			Angle		Velocities	
Designation	Symbol		Designation	Symbol	Positive direction	Designation	Symbol	Linear (component along axis)	Angular
Longitudinal	X	X	Rolling	L	$Y \longrightarrow Z$	Roll	ϕ	u	p
Lateral	Y	Y	Pitching	M	$Z \longrightarrow X$	Pitch	θ	v	q
Normal	Z	Z	Yawing	N	$X \longrightarrow Y$	Yaw	ψ	w	r

Absolute coefficients of moment

$C_l = \frac{L}{qbS}$ (rolling) $\quad C_m = \frac{M}{qcS}$ (pitching) $\quad C_n = \frac{N}{qbS}$ (yawing)

Angle of set of control surface (relative to neutral position), δ. (Indicate surface by proper subscript.)

4. PROPELLER SYMBOLS

D Diameter

p Geometric pitch

p/D Pitch ratio

V' Inflow velocity

V_s Slipstream velocity

T Thrust, absolute coefficient $C_T = \frac{T}{\rho n^2 D^4}$

Q Torque, absolute coefficient $C_Q = \frac{Q}{\rho n^2 D^5}$

P Power, absolute coefficient $C_P = \frac{P}{\rho n^3 D^5}$

C_s Speed-power coefficient $= \sqrt[5]{\frac{\rho V^5}{P n^2}}$

η Efficiency

n Revolutions per second, rps

Φ Effective helix angle $= \tan^{-1}\left(\frac{V}{2\pi r n}\right)$

5. NUMERICAL RELATIONS

1 hp=76.04 kg-m/s=550 ft-lb/sec

1 metric horsepower=0.9863 hp

1 mph=0.4470 mps

1 mps=2.2369 mph

1 lb=0.4536 kg

1 kg=2.2046 lb

1 mi=1,609.35 m=5,280 ft

1 m=3.2808 ft